Measurements of sequences of amino acids 70 and 91 of core region, amino acid 139 of E1 region, and amino acid sequence 2209–2248 of NS5A region of hepatitis C virus

Amino acids 70 and 91 of the core region of HCV, amino acid 139 of the E1 region of HCV, and amino acid sequence of 2209–2248 of the NS5A region of HCV were analyzed by direct nucleotide sequencing of each region according to previous reports.[3,7,8] Hepatitis C virus was defined as wild type for the amino acid sequence of 2209–2248 of the NS5A region when the number of amino acid substitutions in comparison with HCV-J strain[24] was 0 or 1, and as non-wild type when the number of substitutions was greater than 1.

Statistical analyses

Quantitative values are shown as mean ± SD. Between-group differences were analyzed by the chi-square test. Differences in quantitative values between the two groups were analyzed by the Mann-Whitney *U*-test. Multivariate analysis was performed for baseline factors that affected the response to the combination therapy using a logistic regression model. The factors analyzed were age, sex, body weight, history of previous IFN therapy, serum alanine aminotransferase activity, serum aspartate aminotransferase activity, serum gamma-glutamyl transpeptidase, serum alkaline phosphatase, serum albumin, serum total bilirubin, white blood cell count, hemoglobin, platelet count, hepatitis activity grade (A0 and A1 *versus* A2 and A3), grade of liver fibrosis (F0 and F1 *versus* F2 and F3), pretreatment HCV RNA concentration, amino acids 70 and 91 of the HCV core protein, amino acid 139 of HCV E1 protein, and amino acid sequence 2209–2248 of the HCV NS5A protein. All statistical tests were two-tailed; $P < 0.05$ was accepted as statistically significant.

The study protocol was approved by the institutional review board and was in compliance with the Helsinki Declaration. Written informed consent was obtained from all patients prior to the study for use of the laboratory data.

Results

All 107 patients completed the entire treatment duration; no patient dropped-out of the study. Although reduction of PEG-IFN dose and ribavirin dose were experienced by 29 patients (27.1%) and 49 patients (45.8%), respectively, no patient discontinued either PEG-IFN or ribavirin. Eight patients (7.5%) had achieved RVR and 40 patients (37.4%) had achieved cEVR. HCV RNA was undetectable in 77 patients (72.0%) at the end of treatment (ETR). Outcomes following combination therapy were SVR in 39 patients (36.5%), relapse in 38 patients (35.5%), and NR in 30 patients (28.0%). Amino acid position 70 of the HCV protein core region was Arginine (Arg, reportedly associated with a good response to IFN) in 70 patients (65.4%) and Glutamine (Gln, reportedly associated with a poor response) in 29 patients (27.1%). Of the other eight patients, five had Histidine at that position, and in the other three HCV with both Arg and Gln at this position was detected. Amino acid position 91 of the HCV core region was Leucine (Leu, reportedly associated with a good response to IFN) in 76 patients (71.0%) and Methionine (Met, reportedly associated with a poor response) in 29 patients (27.1%). In the remaining two patients, HCV with both Leu and Met at this position was detected. Amino acid position 139 of the HCV E1 region was Threonine (Thr, reportedly associated with a good response to IFN) in 55 patients (51.4%) and Alanine at this position (Ala, reportedly associated with a poor response) in 40 patients (37.4%). From the remaining patients, the amino acid at position 139 was Serine in two patients; in four patients HCV with both Thr and Ala was detected; in HCV from four patients this position was deleted. In two patients we failed to amplify this region. At amino acid range 2209–2248 of the HCV NS5A region, HCV of 61 patients (57.0%) was wild type and that of 46 patients (43.0%) was non-wild type. There was no difference in baseline characteristics, including the rate of patients with reduction of PEG-IFN dose or ribavirin dose, between patients with Arg and Glu at amino acid position 70, between patients with Leu and Met at amino acid position 91, between patients with Thr and Ala at amino acid position 139, and between patients with non-wild type and wild type at amino acids range 2209–2248, respectively (data not shown).

Pretreatment HCV RNA concentration, and reduction in HCV RNA concentration at 24 h after the single administration of conventional interferon and after the start of combination therapy according to amino acid sequences

Pretreatment HCV RNA concentration, the reduction of HCV RNA concentration at 24 h after a single administration test of conventional IFN, and the reduction of HCV RNA concentration at 24 h after the start of combination therapy with PEG-IFN and ribavirin was compared between patients according to the amino acid sequence of the HCV (Table 2). Pretreatment HCV RNA concentration in patients with Arg at position 70 was significantly higher than in those with Gln at that position ($P = 0.0260$). Pretreatment HCV RNA concentration in patients with the wild type sequence at position 2209–2248 was significantly higher than that in patients with the non-wild type sequence ($P = 0.0002$). We found no difference in pretreatment HCV RNA concentration according to the identities of amino acids 91 or 139. The reduction of HCV RNA concentration in patients with Arg at position 70 was significantly more marked than in patients with Gln at that position ($P < 0.0001$). We found no difference in reduction of HCV RNA concentration after a single administration of conventional IFN according to the identities of amino acids 91 or 139, or the 2209–2248 sequence. Similarly, the reduction of HCV RNA concentration at 24 h after the start of combination therapy in patients with Arg at position 70 was significantly greater than that in patients with Gln at position 70 ($P = 0.0025$). We found no difference in reduction of HCV RNA concentration after a single administration of conventional IFN according to the identities of amino acids 91 or 139, or the sequence 2209–2248.

Response to combination therapy with peginterferon and ribavirin

The responses to combination therapy according to amino acid identity are summarized in Table 3. The rates of cEVR, ETR, and SVR were significantly higher in patients with Arg than in those with Gln at position 70 (all $P < 0.0001$), whereas we found no

Table 2 Association between amino acid substitutions and pretreatment HCV RNA concentration, reduction in HCV RNA concentration at 24 h after the single administration of conventional interferon (IFN) alpha-2b, and reduction in HCV RNA concentration at 24 h after the start of combination therapy with peginterferon (PEG-IFN) and ribavirin

	Core: amino acid70		Core: amino acid91	
	Arg ($n = 70$)	Gln ($n = 29$)	Leu ($n = 76$)	Met ($n = 29$)
Pretreatment HCV RNA concentration ($\times 10^3$ IU/mL)	1943 ± 1294	1410 ± 895*	1755 ± 1151	1731 ± 1107
Reduction in HCV RNA concentration at 24 h after single administration ($\log_{10}$)	1.50 ± 0.45	0.95 ± 0.69**	1.41 ± 0.60	1.21 ± 0.49
Reduction in HCV RNA concentration at 24 h after combination therapy ($\log_{10}$)	1.34 ± 0.52	0.97 ± 0.57***	1.25 ± 0.54	1.30 ± 0.60
	E1: amino acid139		NS5A: amino acids 2209–2248	
	Thr ($n = 55$)	Ala ($n = 40$)	Non-wild ($n = 46$)	Wild ($n = 61$)
Pretreatment HCV RNA concentration ($\times 10^3$ IU/mL)	1809 ± 985	1759 ± 1374	1290 ± 851	2115 ± 1205****
Reduction in HCV RNA concentration at 24 h after single administration ($\log_{10}$)	1.34 ± 0.64	1.40 ± 0.53	1.40 ± 0.60	1.32 ± 0.57
Reduction in HCV RNA concentration at 24 h after combination therapy ($\log_{10}$)	1.21 ± 0.53	1.24 ± 0.61	1.29 ± 0.57	1.25 ± 0.55

Mean ± SD.

*$P = 0.0260$; **$P < 0.0001$; ***$P = 0.0025$; ****$P = 0.0002$.

Ala, Alanine; Arg, Arginine; Gln, Glutamine; Leu, Leucine; Met, Methionine; Thr, Threonine.

Table 3 Association between amino acid substitutions and responses to combination therapy with peginterferon and ribavirin

	Core: amino acid70		Core: amino acid91		E1: amino acid139		NS5A: amino acids 2209–2248	
	Arg ($n = 70$)	Gln ($n = 29$)	Leu ($n = 76$)	Met ($n = 29$)	Thr ($n = 47$)	Ala ($n = 34$)	non-wild ($n = 46$)	wild ($n = 61$)
RVR	6 (55.7)	0	6 (43.4)	2 (44.8)	1 (46.8)	4 (38.2)	7 (15.2)	1 (1.6)**
cEVR	39 (55.7)	1 (3.5)*	33 (43.4)	13 (44.8)	22 (46.8)	13 (38.2)	22 (47.8)	24 (39.3)
ETR	58 (82.9)	12 (41.4)*	58 (76.3)	18 (62.1)	36 (76.6)	23 (67.6)	35 (76.1)	42 (68.9)
SVR	33 (47.2)	1 (3.5)*	31 (40.8)	8 (27.6)	19 (40.4)	11 (32.3)	21 (45.7)	18 (29.5)
Relapse	25 (35.6)	11 (37.9)	27 (35.5)	10 (34.5)	17 (36.2)	12 (35.4)	14 (30.4)	24 (39.3)
NR	12 (17.2)	17 (58.6)*	18 (23.7)	11 (37.9)	11 (23.4)	11 (32.3)	11 (23.9)	19 (31.1)

*$P < 0.0001$; **$P = 0.0229$.

Ala, Alanine; Arg, Arginine; cEVR, complete early virologic response; ETR, end-of-treatment response; Gln, Glutamine; Leu, Leucine; Met, Methionine; NR, no response; SVR, sustained virologic response; Thr, Threonine.

difference in the rates of cEVR, ETR, and SVR according to the amino acids at position 91 or 139, or the sequence 2209–2248. In contrast, the NR rate was significantly lower in patients with Arg at position 70 than in those with Gln at that position ($P < 0.0001$). We found no difference in the rates of cEVR, ETR, or SVR according to the identities of amino acids 91 or 139, or the sequence 2209–2248. The results were the same when we focused on 72 treatment-naïve patients (data not shown; see Table S1).

Univariate and multivariate analyses for baseline factors affecting response to combination therapy with peginterferon and ribavirin

Univariate and multivariate analyses were conducted for baseline factors that could affect cEVR, ETR, or SVR. In univariate analysis, serum gamma-glutamyl transpeptidase level ($P = 0.0025$), serum albumin level ($P = 0.0008$), and the amino acid at position 70 of the HCV core region (Arg *versus* Gln, $P < 0.0001$) were significantly associated with cEVR, and platelet count ($P = 0.0707$) was associated with cEVR but not significantly. In multivariate analysis, the identity of amino acid 70 of the HCV core region ($P = 0.0013$), serum albumin level ($P = 0.0265$), and serum gamma-glutamyl transpeptidase level ($P = 0.0308$) independently affected the rate of cEVR (Table 4). Serum gamma-glutamyl transpeptidase level ($P = 0.0004$), serum albumin level ($P = 0.0015$), white blood cell count ($P = 0.0490$), and the identity of amino acid 70 ($P < 0.0001$) were significantly associated with ETR, and serum alkaline phosphatase level ($P = 0.0814$) was associated with ETR but not significantly by univariate analysis. By multivariate analysis, the identity of amino acid 70 ($P = 0.0010$) and serum gamma-glutamyl transpeptidase level ($P = 0.0055$) independently affected ETR (Table 5). In the analysis of factors affecting SVR, serum albumin level ($P = 0.0069$), platelet count ($P = 0.0238$), amino acid 70 of the HCV core region ($P < 0.0001$) were significantly associated with SVR, and serum gamma-glutamyl transpeptidase level ($P = 0.0832$) and the liver fibrosis grade (F0 and F1 *versus* F2 and F3, $P = 0.0998$) were associated

Table 4 Multivariate analysis for factors affecting complete early virologic response

Factor		Parameter estimate	Standard error	X	Odds ratio (95% confidence interval)	*P* value
Gamma-glutamyl transpeptidase	by 1 IU	−0.0162	0.0075	4.66	0.0053 (0.0000–0.3807)	0.0308
Albumin	by 1.0 g/dL	2.3638	1.0650	4.93	181.33 (2.4858–25744)	0.0265
Platelet count	by 1.0 × 10^3/μL	0.0179	0.0554	0.10	1.5106 (0.1243–19.838)	0.7460
Core-70	1: Arginine				1	
	2: Glutamine	−1.7453	0.5429	10.33	0.0305 (0.0016–0.1719)	0.0013

Table 5 Multivariate analysis for factors affecting end-of-treatment response

Factor		Parameter estimate	Standard error	X	Odds ratio (95% confidence interval)	*P* value
Alkaline phosphatase	by 1 IU/L	−0.0028	0.0037	0.59	0.3034 (0.0137–6.6841)	0.4428
Gamma-glutamyl transpeptidase	by 1 IU	−0.0162	0.0058	7.72	0.0053 (0.0001–0.1738)	0.0055
Albumin	by 1.0 g/dL	1.2821	0.7700	2.77	16.787 (0.7440–626.72)	0.0959
White blood cell count	by 1/μL	0.0004	0.0002	3.09	12.603 (0.8685–269.45)	0.0787
Core-70	1: Arginine				1	
	2: Glutamine	−0.9882	0.3006	10.80	0.1386 (0.0400–0.4347)	0.0010

Table 6 Multivariate analysis for factors affecting sustained virologic response

Factor		Parameter estimate	Standard error	X	Odds ratio (95% confidence interval)	*P* value
Gamma-glutamyl transpeptidase	by 1 IU	−0.0015	0.0057	0.07	0.6201 (0.0121–20.764)	0.7962
Albumin	by 1.0 g/dL	1.4230	0.8788	2.62	22.888 (0.6793–1381.2)	0.1054
Platelet count	by 1.0 × 10^3/μL	0.0511	0.0556	0.84	3.2365 (0.2734–44.588)	0.3585
Fibrosis	1: F0/F1				1	
	2: F2/F3	0.0661	0.2976	0.05	1.1413 (0.3557–3.7626)	0.8242
Core-70	1: Arginine				1	
	2: Glutamine	−1.5097	0.5364	7.92	0.0488 (0.0026–0.2661)	0.0049

with SVR but not significantly by univariate analysis. By multivariate analysis, only amino acid 70 of the HCV core region independently affected SVR ($P = 0.0049$, Table 6).

Discussion

In the present study, we validated the association of several reported amino acid substitutions with IFN sensitivity and with the response to combination therapy with PEG-IFN and ribavirin. We found that total rate of SVR in the present study was considerably lower (36.5%) in comparison to previous reports on PEG-IFN and ribavirin combination therapy for patients with HCV genotype 1b. The reason for this was unknown. It could be partly because patients with a history of previous IFN therapy (retreatment cases) were included to the study population, partly because we focused on patients with higher pretreatment HCV RNA concentration, and partly because all patients completed the treatment at 48 weeks without elongation. In addition, more patients with HCV strain resistant to IFN might be included in the study patients, although we enrolled all patients who fulfilled the inclusion criteria.

We found a significant difference in pretreatment HCV RNA concentration according to the amino acid sequence 2209–2248 of the HCV NS5A protein. The original report[3] of an association between the amino acid sequence 2209–2248 of HCV NS5A and the response to IFN monotherapy showed a higher pretreatment HCV RNA concentration in patients with the wild type sequence of the HCV NS5A protein. Our results are in agreement with this result. We found a significant difference in the reduction in HCV RNA concentration at 24 h after a single administration of conventional IFN-alpha, according to the amino acid at position 70 of the HCV core protein. The reduction of HCV RNA concentration after a single administration of conventional IFN was significantly less marked in patients with Gln at position 70. The reduction after a single administration of conventional IFN was considered to reflect the resistance to IFN, and this result suggests a difference in sensitivity to IFN between HCV with Arg at position 70 and that with Gln at position 70. In previous studies, Jessner *et al.*[25,26] and Boulestin *et al.*[27] reported the importance of the decrease in serum HCV RNA concentration at 24 h after a single administration of conventional IFN in distinguishing HCV strains that are resistant to IFN-based antiviral therapy against HCV. We suggest that HCV with Glutamine at position 70 might be resistant to IFN-based therapy.

In the association between amino acid identities and the response to the combination therapy, the identity of the amino acid at position 70 was solely and strongly associated with cEVR, ETR, and SVR. In addition to the effect of the substitution of amino acid 70 of the HCV core region, Akuta *et al.*[8,28,29] reported the effect of the substitution of amino acid 91 of the HCV core region and Donlin *et al.*[7] suggested the effect of the substitution of amino acid 139 of the HCV E1 region on the response to the combination therapy with PEG-IFN and ribavirin in patients infected with HCV genotype 1b. More recently, Mori *et al.*[30] reported the effect of amino acid sequence 2209–2248 of the HCV NS5A region, in addition to the effect of amino acid 70 on the response to combination therapy in Japanese patients with HCV genotype 1b. In contrast to these reports, we did not find an association between these substitutions and the response to the combination therapy. The reason for this discrepancy is unknown. It might be partly because we focused on patients with high pretreatment HCV RNA concentration.

The predictive value for SVR of Arg at position 70 was not high (47.2%). In contrast, the predictive value for the lack of SVR of Gln at position 70 was extremely high (96.5%). The influence of amino acid identity at position 70 was therefore closely related to the resistance to IFN of HCV with Gln at position 70. Recently, Okanoue *et al.* reported the close association of amino acid identity at position 70 not with SVR but with the lack of SVR.[31] Our results supported their findings and, in addition, our results showed the direct resistance to IFN of HCV with Gln at position 70.

There are several limitations of the present study. The patients studied were all Japanese. The effect of amino acid 70 on combination therapy with PEG-IFN and ribavirin should therefore be verified in other ethnicities. Also, all patients studied had high pretreatment HCV RNA concentration ($>100 \times 10^3$ IU/mL). If HCV genotype 1b with amino acid 70 of Gln is resistant to IFN, the lower rates of cEVR, ETR, or SVR will be maintained in patients with HCV genotype 1b but with lower pretreatment HCV RNA concentration. This should also be clarified in the future. In addition, there are no reported mechanisms which could explain the effect of this amino acid substitution on the effectiveness of the combination therapy against HCV. This area should be studied in the future.

In conclusion, the results of the present study show that the substitution of amino acid 70 of the HCV core region was strongly associated with resistance to IFN and was independently associated with the response to the combination therapy with PEG-IFN and ribavirin in Japanese patients with HCV genotype 1b, presumably due to this resistance to IFN of HCV with Gln at position 70. The determination of the identity of amino acid 70 of the HCV core region can be useful for prediction of the resistance to combination therapy in this patient subpopulation, and can be useful for the decision of the indication of this therapy. Further studies in larger patient populations including multiple ethnicities will be needed to validate the significance of these amino acid substitutions and others which have been reported.

References

1 Ghany MG, Strader DB, Thomas DL, Seeff LB. Diagnosis, management, and treatment of hepatitis C: an update. *Hepatology* 2009; **49**: 1335–74.

2 Dienstag JL, McHutchison JG. American Gastroenterological Association technical review on the management of hepatitis C. *Gastroenterology* 2006; **130**: 231–64.

3 Enomoto N, Sakuma I, Asahina Y *et al.* Mutations in the nonstructural protein 5A gene and response to interferon in patients with chronic hepatitis C virus 1b infection. *N. Engl. J. Med.* 1996; **334**: 77–81.

4 Yang SS, Lai MY, Chen DS, Chen GH, Kao JH. Mutations in the NS5A and E2-PePHD regions of hepatitis C virus genotype 1b and response to combination therapy of interferon plus ribavirin. *Liver Int.* 2003; **23**: 426–33.

5 Watanabe H, Nagayama K, Enomoto N *et al.* Amino acid substitutions in PKR-eIF2 phosphorylation homology domain (PePHD) of hepatitis C virus E2 protein in genotype 2a/2b and 1b in Japan and interferon efficacy. *Hepatol. Res.* 2003; **26**: 268–74.

6 Sugihara K, Orito E, Tanaka Y *et al.* Variation in the viral NS5B region in Japanese patients with chronic hepatitis C virus genotype 1 infection. No specific amino acid substitution was identified as determinants of treatment response to interferon/ribavirin combination therapy. *Intervirology* 2006; **49**: 319–26.

7 Donlin MJ, Cannon NA, Yao E *et al.* Pretreatment sequence diversity differences in the full-length hepatitis C virus open reading frame correlate with early response to therapy. *J. Virol.* 2007; **81**: 8211–24.

8 Akuta N, Suzuki F, Kawamura Y *et al.* Prediction of response to pegylated interferon and ribavirin in hepatitis C by polymorphisms in the viral core protein and very early dynamics of viremia. *Intervirology* 2007; **50**: 361–8.

9 Welker MW, Hofmann WP, Welsch C *et al.* Correlation of amino acid variations within nonstructural 4B protein with initial viral kinetics during interferon-alpha-based therapy in HCV-1b-infected patients. *J. Viral. Hepat.* 2007; **14**: 338–49.

10 Pascu M, Martus P, Hohne M *et al.* Sustained virological response in hepatitis C virus type 1b infected patients is predicted by the number of mutations within the NS5A-ISDR: a meta-analysis focused on geographical differences. *Gut* 2004; **53**: 1345–51.

11 Brillet R, Penin F, Hezode C, Chouteau P, Dhumeaux D, Pawlotsky J-M. The nonstructural 5A protein of hepatitis C virus genotype 1b does not contain an interferon sensitivity-determining region. *J. Infect. Dis.* 2007; **195**: 432–41.

12 Chayama K, Tsubota A, Kobayashi M *et al.* Pretreatment virus load and multiple amino acid substitutions in the interferon sensitivity-determining region predict the outcome of interferon treatment in patients with chronic genotype 1b hepatitis C virus infection. *Hepatology* 1997; **25**: 745–9.

13 Squadrito G, Leone F, Sartori M *et al.* Mutations in the nonstructural 5A region hepatitis C virus and response of chronic hepatitis C to interferon alfa. *Gastroenterology* 1997; **113**: 567–72.

14 Khorsi H, Castelain C, Wyseur A *et al.* Mutations of hepatitis C virus 1b NS5A 2209–2248 amino acid sequence do not predict the response to recombinant interferon-alfa therapy in French patients. *J. Hepatol.* 1997; **27**: 72–7.

15 Zeuzem S, Lee JH, Roth WK. Mutations in the nonstructural 5A gene of European hepatitis C virus isolates and response to interferon alfa. *Hepatology* 1997; **25**: 740–4.

16 Hofgartner WT, Polyak SJ, Sullivan DG, Carithers RL Jr, Gretch DR. Mutations in the NS5A gene of hepatitis C virus in North American patients infected with HCV genotype 1a or 1b. *J. Med. Virol.* 1997; **53**: 118–26.

17 Pawlotsky J-M, Germanidis G, Neumann AU, Pellerin M, Frainais P-O, Dhumeaux D. Interferon resistance of hepatitis C virus genotype 1b: relationship to nonstructural 5A gene quasispecies mutations. *J. Virol.* 1998; **72**: 2795–805.

18 Saiz J, Lopez-Labrador F, Dopazo ASJ *et al.* The prognostic relevance of the nonstructural 5A gene interferon sensitivity determining region is different in infections with genotype 1b and 3a isolates of hepatitis C virus. *J. Infect. Dis.* 1998; **177**: 839–47.
19 Sarrazin C, Berg T, Lee J-H *et al.* Improved correlation between multiple mutations within the NS5A region and virological response in European patients chronically infected with hepatitis C virus type 1b undergoing combination therapy. *J. Hepatol.* 1999; **30**: 1004–13.
20 Nakano I, Fukuda Y, Katano Y, Nakano S, Kumada T, Hayakawa T. Why in the interferon sensitivity-determining region (ISDR) system useful in Japan? *J. Hepatol.* 1999; **30**: 1014–22.
21 Chung RT, Monto A, Dienstag JL, Kaplan LM. Mutations in the NS5A region do not predict interferon-responsiveness in American patients infected with genotype 1b hepatitis C virus. *J. Med. Virol.* 1999; **58**: 353–8.
22 McKechnie VM, Mills PR, McCruden ABM. The NS5a gene of hepatitis C virus in patients treated with interferon-α. *J. Med. Virol.* 2000; **60**: 367–78.
23 The French METAVIR Cooperative Study Group. Intraobserver and interobserver variations in liver biopsy interpretation in patients with chronic hepatitis C. *Hepatology* 1994; **20**: 15–20.
24 Kato N, Hijikata M, Ootsuyama Y *et al.* Molecular cloning of the human hepatitis C virus genome from Japanese patients with non-A, non-B hepatitis. *Proc. Natl. Acad. Sci. USA* 1990; **87**: 9524–8.
25 Jessner W, Gschwantler M, Steindl-Munda P *et al.* Primary interferon resistance and treatment response in chronic hepatitis C infection: a pilot study. *Lancet* 2001; **358**: 1241–2.
26 Jessner W, Stauber R, Hackl F *et al.* Early viral kinetics on treatment with pegylated interferon-α-2a in chronic hepatitis C virus genotype 1 infection. *J. Viral. Hepat.* 2003; **10**: 37–42.
27 Boulestin A, Kamar N, Sandres-Saune K *et al.* Twenty-four hour kinetics of hepatitis C virus and antiviral effect of alpha-interferon. *J. Med. Virol.* 2006; **78**: 365–71.
28 Akuta N, Suzuki F, Sezaki H *et al.* Predictive factors of virological non-response to interferon-ribavirin combination therapy for patients infected with hepatitis C virus of genotype 1b and high viral load. *J. Med. Virol.* 2006; **78**: 83–90.
29 Akuta N, Suzuki F, Kawamura Y *et al.* Predictive factors of early and sustained responses to peginterferon plus ribavirin combination therapy in Japanese patients infected with hepatitis C virus genotype 1b: amino acid substitutions in the core region and low-density lipoprotein cholesterol levels. *J. Hepatol.* 2007; **46**: 403–10.
30 Mori N, Imamura M, Kawakami Y *et al.* Randomized trial of high-dose interferon-alpha-2b combined with ribavirin in patients with chronic hepatitis C: correlation between amino acid substitutions in the core/NS5A region and virological response to interferon therapy. *J. Med. Virol.* 2009; **81**: 640–9.
31 Okanoue T, Itoh Y, Hashimoto H *et al.* Predictive values of amino acid sequences of the core and NS5A regions in antiviral therapy for hepatitis C: a Japanese multi-center study. *J. Gastroenterol.* 2009; **44**: 952–63.

Supporting information

Additional Supporting Information may be found in the online version of this article:

Table S1. Association between amino acid substitutions and responses to combination therapy with peginterferon and ribavirin in treatment-naïve patients.

Please note: Wiley-Blackwell are not responsible for the content or functionality of any supporting materials supplied by the authors. Any queries (other than missing material) should be directed to the corresponding author for the article.

Liver INTERNATIONAL
OFFICIAL JOURNAL OF THE INTERNATIONAL ASSOCIATION FOR THE STUDY OF THE LIVER

Liver International ISSN 1478-3223

CLINICAL STUDIES

Impact of amino acid substitutions in the hepatitis C virus genotype 1b core region on liver steatosis and hepatic oxidative stress in patients with chronic hepatitis C

Yoshihiko Tachi[1], Yoshiaki Katano[1], Takashi Honda[1], Kazuhiko Hayashi[1], Masatoshi Ishigami[1], Akihiro Itoh[1], Yoshiki Hirooka[1], Isao Nakano[1], Youichi Samejima[2] and Hidemi Goto[1]

1 Department of Gastroenterology, Nagoya University School of Medicine, Nagoya, Aichi, Japan
2 Department of Gastroenterology, Kakegawa City General Hospital, Kakegawa, Shizuoka, Japan

Keywords
8-hydroxy-2′-deoxyguanosine – amino acid substitutions – hepatitis C virus – glutamine – liver steatosis – methionine – oxidative stress

Correspondence
Yoshiaki Katano, Department of Gastroenterology, Nagoya University Graduate School of Medicine, 65, Tsurumai-cho, Syowa-ku, Nagoya, Aichi 466-8550, Japan
Tel: +81 52 744 2169
Fax: +81 52 744 2178
e-mail: ykatano@med.nagoya-u.ac.jp

Received 31 July 2009
Accepted 13 October 2009

DOI:10.1111/j.1478-3231.2009.02164.x

Abstract

Background: Liver steatosis and hepatic oxidative stress are the histopathological features of chronic hepatitis C. Hepatitis C virus (HCV) genotype 1 core protein induces hepatic steatosis and reactive oxygen species production in transgenic mice. The amino acid substitutions in the HCV core region appear to be related to hepatocarcinogenesis. *Aims:* The aim of this study was to clarify the impact of mutations in the HCV core region on oxidative stress and lipid metabolism in patients with chronic hepatitis C. *Methods:* Sixty-seven patients (35 men, 32 women; mean age, 58.4 ± 10.2 years) with chronic hepatitis C with high titres (> 5 log IU/ml) were enrolled. Substitutions in amino acids 70, 75 and 91 of the HCV genotype 1b core region, the percentage of hepatic steatosis, and hepatic 8-hydroxy-2′-deoxyguanosine (8-OHdG) levels were investigated in all patients. Urinary 8-OHdG levels were measured in 35 patients. *Results:* Body mass index, alanine aminotransferase, γ-glutamyl transferase, and triglyceride levels and substitutions of amino acid 70/Q (glutamine) were significantly associated with the presence of steatosis on univariate analysis. Multivariate analysis showed that substitution of amino acid 70 of glutamine and triglyceride levels were the independent factors related to liver steatosis. Hepatic and urinary 8-OHdG levels were significantly higher in patients with methionine at amino acid 91 of the HCV core region than in those with leucine. *Conclusion:* Substitutions in the amino acids of the HCV genotype1b core region are associated with hepatic steatosis and oxidative stress in patients with chronic hepatitis C.

Hepatitis C virus (HCV) infection is widespread, with 170 million carriers worldwide (1). HCV infection leads to chronic hepatitis, cirrhosis and hepatocellular carcinoma (HCC), and it is a major global health issue. HCV, a hepatotropic Flavivirus, is formed by a positive, single-stranded RNA genome of about 9600 nucleotides that contains an open reading frame. HCV has two structural proteins, core protein and envelope protein. HCV core protein induces oxidative stress, which contributes to the pathogenesis of chronic hepatitis C. Transgenic mice that express HCV core protein develop hepatic steatosis and increased reactive oxygen species (ROS) production without inflammation (2, 3). Oxidative stress plays an important role in patients with chronic hepatitis C. It has been reported that 8-hydroxy-2′-deoxyguanosine (8-OHdG) reflects oxidative DNA damage by hydroxyl radicals (4, 5) and increases in the liver tissue and circulating leucocytes of patients with chronic hepatitis C (6–8). Hepatic oxidative stress is associated with the progression of fibrosis and increases the risk for HCC (9, 10). Therefore, the evaluation of oxidative stress in patients with chronic hepatitis C would be useful for understanding the pathogenesis of hepatitis. Not only hepatic oxidative stress but also lipid metabolism abnormalities, such as liver steatosis, are the histopathological features of human chronic hepatitis C. Several factors, such as metabolic syndrome, obesity and a high body mass index (BMI) have an influence on liver steatosis in chronic hepatitis C patients (11). Viral factors such as HCV genotype 3 and core protein, as well as host factors, contribute to the development of hepatic steatosis (12, 13). Therefore, several studies demonstrated that HCV core protein has close relationships both with induction of ROS and lipid metabolism, such as liver steatosis (14). However, these associations are not fully understood. Recently, some studies have indicated that amino acid substitutions in the HCV core region of genotype 1b were related to response to interferon

(IFN)–ribavirin combination therapy (15, 16) and insulin resistance (17). We speculated that these mutations in the HCV core region may be related to hepatic steatosis and oxidative stress in chronic hepatitis C patients. To investigate this hypothesis, we analysed the impact of amino acid substitutions in the HCV core region on histological hepatic steatosis and hepatic and urinary 8-OHdG levels.

Methods

Patients

Sixty-seven patients with chronic hepatitis C who were treated at Kakegawa City General Hospital between December 2004 and December 2008 were enrolled. The patients were 35 men and 32 women, with a mean age of 58.4 years. The exclusion criteria were: co-infection with hepatitis B virus and human immunodeficiency virus, drug addiction, alcoholism, autoimmune hepatitis, coexisting serious psychiatric or mental illness and pregnancy. All patients were genotype 1b with high titres ($>$ 5 log IU/ml), and they were treated using a combination therapy with pegylated IFN and ribavirin. Peginterferon-α-2b (PegIntron; Schering Plough, Osaka, Japan) was given once a week for 48–72 weeks. Oral ribavirin (Rebetol; Schering Plough) was given at a dose of 600 mg/day to patients who weighed $\leq$ 60 kg and at a dose of 800 mg/day to those who weighed $>$ 60 kg during the treatment period. Before therapy, blood and urine were sampled in the morning of the day of the liver biopsy after overnight fasting.

Liver histology

Ultrasound-guided percutaneous needle liver biopsies were performed in all 67 patients. All liver biopsies were reviewed by a pathologist who was blinded to the clinical and laboratory findings. Liver biopsy specimens were classified in terms of fibrosis and necroinflammatory activity according to the classification by Desmet *et al.* (18). Findings of steatosis were assessed according to the percentage of hepatocytes containing fat droplets and graded as follows: 0 (no steatosis), 1 ($<$ 33% of hepatocytes affected), 2 (33–66% of hepatocytes affected) and 3 ($>$ 66% of hepatocytes affected).

Histological examination for 8-hydroxy-2′-deoxyguanosine in the liver

Histological 8-OHdG in the liver was quantified using liver biopsy samples taken before IFN therapy, as reported previously (19). The sections were stained using mouse monoclonal antibody against 8-OHdG (5 μg/ml; Japan Institute for the Control of Aging, Fukuroi, Shizuoka, Japan). Nuclei positive for 8-OHdG were counted in two non-overlapping randomly selected fields. The degree of oxidative stress of the liver was expressed by the average percentage of hepatocytes with 8-OHdG-positive nuclei in the two fields.

Urinary 8-hydroxy-2′-deoxyguanosine

Urine samples were collected before treatment in 35 of 67 patients. Urinary 8-OHdG levels were measured in 35 patients. The 8-OHdG concentration was determined using an enzyme-linked immunosorbent assay kit (Japan Institute for the Control of Aging; Nikken SEIL Corporation; Fukuroi, Shizuoka, Japan), and the urinary creatinine concentration was determined by a standard automated colorimetric assay. Then, urinary 8-OHdG was normalized for the urinary creatinine level, and it was presented as the urinary [8-OHdG (ng/ml)/creatinine (mg/ml)] ratio.

Amino acid substitutions in the hepatitis C virus core region of genotype 1b

Direct sequencing of the core region was carried out as reported previously but with modifications (20). In brief, RNA was extracted from 140 μl sera with a commercial kit (QIAamp viral RNA kit; Qiagen, Valencia, CA, USA) and dissolved in 50 μl diethylpyrocarbonate-treated water. Ten nanograms of RNA were used for reverse transcription with oligo and random hexamer primers with a commercial kit (iScript cDNA synthesis kit; Bio-Rad, Hercules, CA, USA). The core region was amplified by nested PCR. In brief, each 50 μl PCR reaction contained 100 nM of each primer, 1 ng template cDNA, 5 μl GeneAmp × 10 PCR buffer, 2 μl dNTPs and 1.25 U AmpliTaq Gold (Applied Biosystems, Foster City, CA, USA). Primer sequences were as follows: sense, 5′-GGG AGGTCTCGTAGACCGTGCACCATG-3′ and antisense, 5′-GAGMGGKATRTACCCCATGAGRTCGGC-3′. Amplification conditions consisted of 10 min at 94 °C followed by 40 cycles at 94 °C for 10 s, 55 °C for 30 s and 72 °C for 30 s in a thermal cycler (GeneAmp PCR System 9700; Applied Biosystems). The second PCR was performed in the same reaction buffer with the first-round PCR product as template, the sense primer 5′-AGACC GTGCACCATGAGCAC-3′ and antisense primer 5′-TAC GCCGGGGGTCAKTRGGGCCCCA-3′. PCR products were separated by electrophoresis on 2% agarose gels, stained with ethidium bromide and visualized under ultraviolet light. PCR products were then purified and sequenced with the second-round PCR primers with a dye terminator sequencing kit (BigDye Terminator v1.1 Cycle sequencing kit; Applied Biosystems) and an ABI 310 DNA sequencer (Applied Biosystems).

Statistical analysis

Quantitative values were expressed as means ± SD or medians. Each data set was first evaluated for normality of distribution by the Shapiro–Wilk test to decide whether a non-parametric rank-based analysis or a parametric analysis should be used. Between-group

differences in mean quantitative values were analysed using the Kruskal–Wallis *H*-test, and differences between two groups in non-parametric data were analysed by the Mann–Whitney *U*-test, χ^2-test and Fisher's exact probability test. Differences in parametric data were analysed using the paired *t*-test. Correlations between variables were tested using Spearman's rank-correlation analysis. The parameters that were found to be significant on univariate analysis were further processed through multivariate logistic regression analysis. All *P* values were two tailed, and $P < 0.05$ was considered statistically significant. Statistical analysis was carried out using SPSS version 16.0 for WINDOWS (SPSS Inc., Chicago, IL, USA).

Results

The patients' clinical characteristics are shown in Table 1. Comparisons of clinical characteristics according to the presence of steatosis are shown in Table 2. There were significant positive associations between the presence of steatosis and BMI, alanine aminotransferase levels, γ-glutamyltransferase levels, triglyceride levels and substitutions of amino acid 70. On multivariate logistic regression analysis, factors associated with steatosis were substitutions of amino acid 70/Q (glutamine) and triglyceride levels (Table 3).

Table 1. Clinical characteristics ($n = 67$)

Characteristics	
Age (years)	58.4 ± 10.2
Gender (male/female)	35/32
Body mass index	21.9 ± 2.8
Laboratory data	
AST (IU/L)	61.0 ± 36.2
ALT (IU/L)	62.4 ± 37.4
γ-GTP (IU/L)	52.9 ± 45.4
Cholesterol (mg/dl)	181.14 ± 39.38
Triglycerides (mg/dl)	92.69 ± 41.33
Platelet count (x 10^4/ml)	16.4 ± 4.3
Serum ferritin (ng/ml)	156.8 ± 144.9
HOMA-IR	3.55 ± 4.58
Liver histology	
Inflammatory activity (A0/A1/A2/A3)	16/44/6/1
Fibrosis staging (F0/F1/F2/F3/F4)	10/28/15/14/0
Liver steatosis (Grade 0/1/2/3)	22/40/5/0
Liver steatosis (%)	8.43 ± 12.1
Hepatic 8-OHdG (absent/present)	19/48
Hepatic 8-OHdG (%)	42.67 ± 31.56
Urinary 8-OHdG (ng/mg Cr)*	10.99 ± 5.27
Amino acid substitutions of HCV core region	
aa 70 (arginine/glutamine/histidine)	42/23/2
aa 75 (threonine/alanine/serine/valine)	26/38/2/1
aa 91 (leucine/methionine)	43/24

Data are expressed as mean ± SD, and the numbers represent number of patients.

*35 patients were available.

ALT, alanine aminotransferase; AST, aspartate aminotransferase; core aa, core amino acid; γ-GTP, γ-glutamyltransferase; HCV, hepatitis C virus; HOMA-IR, the index of homeostasis model assessment-insulin resistance; 8-OHdG, 8-hydroxy-2′-deoxyguanosine.

Table 4 shows correlations between hepatic/urinary 8-OHdG levels and amino acid substitutions at positions 70/75/91 in the HCV core region. The hepatic 8-OHdG levels were significantly lower ($P = 0.0453$) in the patient group without methionine (non-M) than in the patient group with methionine (M) at amino acid 91 of the HCV core region. The urinary 8-OHdG levels were significantly lower ($P = 0.0112$) in the patient group without M than in the patient group with M at amino acid 91 of the HCV core region. There were significant correlations between expression of hepatic and urinary 8-OHdG levels. We defined absence of oxidative stress as 8-OHdG $\leq$ 10%, while 8-OHdG > 10% indicated the presence of oxidative stress. Substitutions at amino acid 91/M were detectable in 22 of 48 (45.8%) patients with hepatic oxidative stress, but in only two of the 19 (10.5%) patients without hepatic oxidative stress. There were significant positive associations between the presence of hepatic oxidative stress and substitutions of amino acid 91/M ($P = 0.00977$). A sustained virological response (SVR) was achieved by 28 of 59 (47.5%) patients. In the patient group with non-Q (arginine or histidine) at amino acid 70, SVR was achieved by 24 of 40 (60%) patients. In the patient group with Q (glutamine) at amino acid 70, SVR was achieved by four of 19 (21.1%) patients. There was a significantly higher rate of SVR ($P = 0.0117$) in the patient group with non-Q (arginine or histidine) than in the patient group with Q (glutamine) at amino acid 70. There were no significant differences in substitutions of other amino acids (75, 91) on the efficacy of treatment.

We retrospectively assessed changes in urinary 8-OHdG levels before and after treatment in 18 patients. Twelve patients had achieved SVR, another six patients were non-virological response (NVR). The urinary 8-OHdG levels were significantly decreased in SVR patients after treatment ($P = 0.0164$). On the other hand, no significant change was observed in NVR patients.

Discussion

A high prevalence (67%) of steatosis was found among patients with chronic hepatitis C. Liver steatosis is one of the most important histopathological features in patients with chronic hepatitis C. However, it remains uncertain whether liver steatosis is related directly to the virus or is secondary to host factors. It has been suggested that HCV genotype 3 is closely associated with liver steatosis (21). However, in patients who did not have genotype 3, it has been reported that liver steatosis occurred through oxidative stress and insulin resistance with HCV infection (22–24). A recent report has shown that only HCV core protein is necessary for liver steatosis, and the interaction of HCV core protein leads to the activation of the sterol regulatory element-binding protein – 1c promoter and development of liver steatosis (25–27).

Table 2. Clinical characteristic of the patients according to the prevalence of steatosis ($n = 67$)

Characteristics	Steatosis absent ($n = 22$)	Steatosis present ($n = 45$)	*P* values
Age (years)	57.14 ± 12.87	59.06 ± 8.69	NS
Gender (male/female)	12/10	23/22	NS
Body mass index	20.57 ± 2.46	22.57 ± 2.79	0.0080
AST	48.45 ± 20.77	66.96 ± 40.62	NS
ALT	48.09 ± 27.95	69.40 ± 39.59	0.023
γ-GTP	35.36 ± 23.0	61.49 ± 51.03	0.0067
Cholesterol	181.59 ± 40.72	180.41 ± 39.15	NS
Triglycerides	80.91 ± 39.21	98.59 ± 41.53	0.043
Platelet count	16.35 ± 4.93	15.09 ± 3.93	NS
HOMA-IR	1.79 ± 0.87	4.29 ± 5.43	0.064
Serum ferritin	134.21 ± 164.57	167.87 ± 134.84	0.093
Hepatic 8-OhdG (absent/present)	7/15	12/33	NS
Substitutions of aa			
aa 70 (non-Q/Q)	20/2	24/21	0.00243
aa 75 (non-A/A)	12/10	14/31	NS
aa 91 (non-M/M)	14/8	29/16	NS
Inflammatory activity (A0/A1/A2/A3)	(8/13/0/1)	(8/31/6/0)	NS
Fibrosis staging (F0/F1/F2/F3/F4)	(4/11/3/4/0)	(6/17/12/10/0)	NS

Data analysis were performed using Mann–Whitney *U*-test, χ^2-test and Fisher's exact probability test and Kruskal–Wallis *H*-test.
ALT, alanine aminotransferase; AST, aspartate aminotransferase; γ-GTP, γ-glutamyltransferase, HOMA-IR, the index of homeostasis model assessment-insulin resistance; NS, not significant; 8-OHdG, 8-hydroxy-2′-deoxyguanosine.

Table 3. Associations with steatosis found in multivariable logistic regression ($n = 67$)

Characteristics	Category	Odds ratio	95% CI	*P* values
BMI	1: < 22.5 2: ≥22.5	2.069	0.540–7.928	0.289
Core amino acid 70 substitution	1: 70 non-Q 2: 70 Q	7.336	1.178–45.685	0.033
ALT	1: < 44 2: ≥44	3.012	0.661–13.729	0.154
γ-GTP	1: < 26 2: ≥26	1.923	0.406–9.097	0.410
Triglycerides	1: < 86 2: ≥86	4.025	1.038–15.612	0.044
Serum ferritin	1: < 96 2: ≥96	1.306	0.311–5.489	0.715

ALT, alanine aminotransferase; BMI, body mass index; 95% CI, 95% confidence interval; γ-GTP, γ-glutamyltransferase.

Thus, HCV core protein interacts with several pathways, including lipid metabolism, and could be a factor causing liver steatosis. HCV genotype 3 induced much more steatosis than genotype 1. Sequence analysis to identify the mutations that are associated with steatosis in genotype 3 has been performed, and it has been reported that amino acids 164, 182 and 186 of the HCV genotype 3 core region affect lipid metabolism (28, 29).

Hepatic steatosis in HCV genotype 1 and the expression of HCV core protein were evaluated, and the sequence variations related to steatosis were unclear. We found that there was a significant association between the prevalence of steatosis and substitutions of amino acid 70 on multivariate logistic regression analysis. Substitutions at amino acid 70/Q were detectable in 21 of 45 (46.7%) patients with steatosis, but only in two of the 22 (9.1%) patients without steatosis ($P = 0.00243$). The major amino acid 70 of genotype 3a was arginine, which defined the non-Q group. Thus, HCV genotype 1b with the amino acid 70/Q, which frequently caused steatosis, was not common in genotype 3a. HCV genotype 1b with 70/Q would enhance fatty acid synthase promoter or accelerate intracellular lipid accumulation as well as genotype 3, but further investigations are needed to confirm these speculations. Although the effect of substitutions of the core amino acid 70 is unclear, liver steatosis was increased by substitutions of the amino acid 70/Q of HCV genotype 1b core region.

The other factor that was related to liver steatosis was triglyceride levels. Lipid metabolism should be associated with liver steatosis, and triglyceride levels would be expected to be an index of the degree of liver steatosis. Several investigators have reported that host factors such as high BMI, obesity and insulin resistance were related

Table 4. Hepatic 8-OHdG ($n = 67$) and urinary 8-OHdG ($n = 35$) according to amino acid substitutions in core region

	Amino acid 70		Amino acid 75		Amino acid 91	
	Non-Q	Q	Non-A	A	Non-M	M
Hepatic 8-OhdG (%)	42.71 ± 31.0	42.60 ± 33.2	47.54 ± 29.5	39.95 ± 32.7	37.14 ± 31.1	52.58 ± 30.6
P values	NS		NS		$P = 0.045$	
Urinary 8-OhdG (ng/ml Cr)	10.26 ± 4.9	12.56 ± 5.9	12.14 ± 7.3	10.39 ± 3.9	9.31 ± 3.7	15.87 ± 6.3
P values	NS		NS		$P = 0.011$	

Data are expressed as mean ± SD. Data analysis were performed using Mann–Whitney *U*-test.
Core amino acids: Q, glutamine; A, alanine; M, methionine.
NS, not significant; 8-OHdG, 8-hydroxy-2′-deoxyguanosine.

to steatosis in patients with chronic hepatitis C. The prevalence of steatosis was significantly associated with increased BMI in the present study ($P = 0.0080$). There was a slight association with an increased index of homeostasis model assessment-insulin resistance, though this was not statistically significant ($P = 0.064$). The prevalence of steatosis (67%) observed was compatible with previous reports (30). However, the BMI (mean = 21.9) in the present study was less than in previous reports, and there were no patients with a BMI over 30; thus, the influence of obesity on liver steatosis was avoided. Although the BMI was low, the fact that the same level of liver steatosis was observed in the present study as in the past shows that HCV has an influence on liver steatosis that is independent of the BMI.

The substitutions of amino acid 91 of the HCV genotype 1b core region were associated with oxidative stress. Previous studies have shown that expression of the HCV core protein causes oxidative injury as a direct effect on mitochondria and increased ROS production in transgenic mice (14). One clinical study revealed that the rates of hepatocarcinogenesis in patients infected with the wild type of HCV core region were lower than in those with the mutant type (31). These results demonstrated that oxidative stress was related to substitutions of the HCV core region and the expression of HCV core protein. However, the effects of substitutions in the core region on core proteins are unknown. This might be due to differences in function through changes in the secondary structure or in the regulation of the expression level of HCV core protein and metabolic pathways. Further experiments are needed to clarify the mechanisms of these mutations.

Anti-oxidative stress treatment would be an option, especially for patients with substitution of amino acid 91/M of the HCV core region. Urinary 8-OHdG is a useful indicator that reflects systemic oxidative stress, as does hepatic 8-OHdG (32). Urinary 8-OHdG was superior to hepatic 8-OHdG because it is easy to measure. Therefore, serial urinary 8-OHdG levels in patients who received IFN therapy were evaluated, and it was confirmed that patients who achieved SVR had reduced oxidative stress. While the patient is on anti-oxidative stress treatment, the urinary 8-OHdG level would be a useful biomarker of oxidative stress for routine clinical use.

Oxidative stress as measured by 8-OHdG levels and hepatic steatosis were the common characteristics of chronic hepatitis C. Oxidative stress and hepatic steatosis were independent factors, but they are related; oxidative stress and hepatic steatosis have similar relationships with the HCV core region but different mutations are involved. The HCV core would be a key to the solution of the mechanism of HCV infection. Large clinical studies and formal basic research are needed to clarify these issues.

In conclusion, our results indicate that substitutions in amino acid 70 of the HCV core region were associated with hepatic steatosis, and similar relationships between substitutions in amino acid 91 and hepatic oxidative stress exist. Therefore, HCV core protein would be one of the most important factors for the development of liver steatosis and hepatic oxidative stress in chronic hepatitis C patients.

References

1. Seeff LB. Natural history of chronic hepatitis C. *Hepatology* 2002; **36**: S35–46.
2. Moriya K, Yotsuyanagi H, Shintani Y, *et al.* Hepatitis C virus core protein induces hepatic steatosis in transgenic mice. *J Gen Virol* 1997; **78**(Part 7): 1527–31.
3. Moriya K, Nakagawa K, Santa T, *et al.* Oxidative stress in the absence of inflammation in a mouse model for hepatitis C virus-associated hepatocarcinogenesis. *Cancer Res* 2001; **61**: 4365–70.
4. Kasai H, Nishimura S. Hydroxylation of deoxyguanosine at the C-8 position by ascorbic acid and other reducing agents. *Nucleic Acids Res* 1984; **12**: 2137–45.
5. Floyd RA, West MS, Eneff KL, *et al.* Hydroxyl free radical mediated formation of 8-hydroxyguanosine in isolated DNA. *Arch Biochem Biophys* 1988; **262**: 266–72.
6. Shimoda R, Nagashima M, Sakamoto M, *et al.* Increased formation of oxidative DNA damage, 8-hydroxydeoxyguanosine, in human livers with chronic hepatitis. *Cancer Res* 1994; **54**: 3171–72.
7. Farinati F, Cardin R, Degan P, *et al.* Oxidative DNA damage in circulating leukocytes occurs as an early event in chronic HCV infection. *Free Radic Biol Med* 1999; **27**: 1284–91.

8. Cardin R, Saccoccio G, Masutti F, *et al.* DNA oxidative damage in leukocytes correlates with the severity of HCV-related liver disease: validation in an open population study. *J Hepatol* 2001; **34**: 587–92.
9. Ichiba M, Maeta Y, Mukoyama T, *et al.* Expression of 8-hydroxy-2′-deoxyguanosine in chronic liver disease and hepatocellular carcinoma. *Liver Int* 2003; **23**: 338–45.
10. Tanaka H, Fujita N, Sugimoto R, *et al.* Hepatic oxidative DNA damage is associated with increased risk for hepatocellular carcinoma in chronic hepatitis C. *Br J Cancer* 2008; **98**: 580–6. Epub 29 January 2008.
11. Lonardo A, Adinolfi LE, Loria P, *et al.* Steatosis and hepatitis C virus: mechanisms and significance for hepatic and extrahepatic disease. *Gastroenterology* 2004; **126**: 586–97 (review).
12. Westin J, Nordlinder H, Lagging M, *et al.* Steatosis accelerates fibrosis development over time in hepatitis C virus genotype 3 infected patients. *J Hepatol* 2002; **37**: 837–42.
13. Fujie H, Yotsuyanagi H, Moriya K, *et al.* Steatosis and intrahepatic hepatitis C virus in chronic hepatitis. *J Med Virol* 1999; **59**: 141–5.
14. Okuda M, Li K, Beard MR, *et al.* Mitochondrial injury, oxidative stress, and antioxidant gene expression are induced by hepatitis C virus core protein. *Gastroenterology* 2002; **122**: 568–71.
15. Akuta N, Suzuki F, Sezaki H, *et al.* Association of amino acid substitution pattern in core protein of hepatitis C virus genotype 1b high viral load and non-virological response to interferon–ribavirin combination therapy. *Intervirology* 2005; **48**: 372–80.
16. Donlin MJ, Cannon NA, Yao E, *et al.* Pretreatment sequence diversity differences in the full-length hepatitis C virus open reading frame correlate with early response to therapy. *J Virol* 2007; **81**: 8211–24. Epub 23 May 2007.
17. Akuta N, Suzuki F, Hirakawa M, *et al.* Amino acid substitutions in the hepatitis C virus core region of genotype 1b are the important predictor of severe insulin resistance in patients without cirrhosis and diabetes mellitus. *J Med Virol* 2009; **81**: 1032–9.
18. Desmet VJ, Gerber M, Hoofnagle JH, *et al.* Classification of chronic hepatitis: diagnosis, grading and staging. *Hepatology* 1994; **19**: 1513–20.
19. Horiike S, Kawanishi S, Kaito M, *et al.* Accumulation of 8-nitroguanine in the liver of patients with chronic hepatitis C. *J Hepatol* 2005; **43**: 403–10.
20. Ohno O, Mizokami M, Wu RR, *et al.* New hepatitis C virus (HCV) genotyping system that allows for identification of HCV genotypes 1a, 1b, 2a, 2b, 3a, 3b, 4, 5a, and 6a. *Clin Microbiol* 1997; **35**: 201–7.
21. Rubbia-Brandt L, Quadri R, Abid K, *et al.* Hepatocyte steatosis is a cytopathic effect of hepatitis C virus genotype 3. *J Hepatol* 2000; **33**: 106–15.
22. Vidali M, Tripodi MF, Ivaldi A, *et al.* Interplay between oxidative stress and hepatic steatosis in the progression of chronic hepatitis C. *J Hepatol* 2008; **48**: 399–406. Epub 3 December 2007.
23. Cammà C, Bruno S, Di Marco V, *et al.* Insulin resistance is associated with steatosis in nondiabetic patients with genotype 1 chronic hepatitis C. *Hepatology* 2006; **43**: 64–71.
24. Conjeevaram HS, Kleiner DE, Everhart JE, *et al.* Race, insulin resistance and hepatic steatosis in chronic hepatitis C. *Hepatology* 2007; **45**: 80–7.
25. Miyanari Y, Atsuzawa K, Usuda N, *et al.* The lipid droplet is an important organelle for hepatitis C virus production. *Nat Cell Biol* 2007; **9**: 1089–97. Epub 26 August 2007. Erratum in: *Nat Cell Biol* 2007 October; **9**(10): 1216.
26. Moriya K, Todoroki T, Tsutsumi T, *et al.* Increase in the concentration of carbon 18 monounsaturated fatty acids in the liver with hepatitis C: analysis in transgenic mice and humans. *Biochem Biophys Res Commun* 2001; **281**: 1207–12.
27. Moriishi K, Mochizuki R, Moriya K, *et al.* Critical role of PA28gamma in hepatitis C virus-associated steatogenesis and hepatocarcinogenesis. *Proc Natl Acad Sci USA* 2007; **104**: 1661–6. Epub 18 January 2007.
28. Jackel-Cram C, Babiuk LA, Liu Q. Up-regulation of fatty acid synthase promoter by hepatitis C virus core protein: genotype-3a core has a stronger effect than genotype-1b core. *J Hepatol* 2007; **46**: 999–1008.
29. Jhaveri R, McHutchison J, Patel K, *et al.* Specific polymorphisms in hepatitis C virus genotype 3 core protein associated with intracellular lipid accumulation. *J Infect Dis* 2008; **197**: 283–91.
30. Bach N, Thung SN, Schaffner F. The histological features of chronic hepatitis C and autoimmune chronic hepatitis: a comparative analysis. *Hepatology* 1992; **15**: 572–7.
31. Akuta N, Suzuki F, Kawamura Y, *et al.* Amino acid substitutions in the hepatitis C virus core region are the important predictor of hepatocarcinogenesis. *Hepatology* 2007; **46**: 1357–64.
32. Cooke MS, Evans MD, Dizdaroglu M, *et al.* Oxidative DNA damage: mechanisms, mutation, and disease. *FASEB J* 2003; **17**: 1195–214.

Cancer Gene Therapy (2012) 19, 637–643

www.nature.com/cgt

ORIGINAL ARTICLE

Effects of interferon-α-transduced tumor cell vaccines and blockade of programmed cell death-1 on the growth of established tumors

R Omori[1], J Eguchi[1], K Hiroishi[1], S Ishii[1], A Hiraide[1], M Sakaki[1], H Doi[1], A Kajiwara[1], T Ito[1], M Kogo[2] and M Imawari[1]

Interferon-alpha (IFN-α) has strong antitumor effects, and IFN-α gene therapy has been used clinically against some cancers. In this study, we evaluated the efficacy of the combination of IFN-α-transduced tumor cell vaccines and programmed cell death 1 (PD-1) blockade, and investigated the mechanisms of the antitumor effects of the combined therapy. A poorly immunogenic murine colorectal cancer cell line, MC38, was transduced to overexpress IFN-α. In a therapeutic model, parental tumor-bearing mice were inoculated with MC38-IFNα cells and an anti-PD-1 antagonistic antibody. Analyses of immunohistochemistry and tumor-specific lysis were performed. The outgrowth of the established tumors was significantly reduced in mice treated with the combination of IFN-α and anti-PD-1. Immunohistochemical analyses of the therapeutic model showed marked infiltration of $CD4^+$ cells and $CD8^+$ cells in the established MC38 tumors of mice treated with both IFN-α and anti-PD-1. Significant tumor-specific cytolysis was detected when splenocytes of mice that were treated with both IFN-α and anti-PD-1 were used as effector cells. These results suggest that blockade of the PD-1 PD-ligand enhanced the Th1-type antitumor immune responses induced by IFN-α. The combination of IFN-α gene-transduced tumor cell vaccines and PD-1 blockade may be a possible candidate for a cancer vaccine for clinical trials.

Cancer Gene Therapy (2012) **19,** 637–643; doi:10.1038/cgt.2012.42; published online 13 July 2012

Keywords: colorectal cancer; cytotoxic T lymphocyte; immunotherapy; interferon-alpha; programmed cell death-1; tumor-based vaccine

INTRODUCTION

Cellular immune responses are thought to be impaired in patients with advanced malignant tumors, and tumors are thought to escape immune surveillance of patients by several mechanisms.[1,2] To overcome the immune suppression or immune escape of patients with malignant tumors, novel approaches for inducing a strong cellular immune response are needed in such patients. Several studies have revealed that the cytokine gene transduction of tumor cells induces potent antitumor immune responses without systemic adverse effects in murine models. The subcutaneous injection of the transduced cells can induce a local inflammation at the site of tumor by the accumulation of inflammatory cells, such as activated natural killer (NK) cells, macrophages, dendritic cells and T lymphocytes.[3–6] As a result of these phenomena, the clinical application of a vaccination using gene-transduced tumor cells as a vehicle to deliver cytokines is attractive.

Interferon-alpha (IFN-α) has many biologic effects, including the enhancement of IFN-α/β production,[7,8] an antiviral function, the inhibition of cell growth and antiangiogenesis.[9] IFN-α upregulates the expression of major histocompatibility complex class I molecules on the cell surface, enhances the proliferation of type-I helper T cells (Th1),[10] and has an important role in the generation of cytotoxic T lymphocytes (CTLs) in specific antitumor immune responses.[11] We previously reported that IFN-α-expressing tumor cells promote the survival of tumor-specific CTLs by preventing apoptosis,[12] and in addition, the combination of IFN-α gene therapy and either interleukin (IL)-4 or IL-12 gene therapy was found to suppress the outgrowth of established tumors.[13,14] Based on these immunomodulating effects of IFN-α, it has been used to treat patients with tumors, such as melanoma, renal cell carcinoma and leukemia.

The programmed cell death-1 (PD-1) protein was first described as a member of the B7 family of costimulatory molecules that modulate T-cell antigen-specific receptor signaling and control T-cell activation, inactivation and survival.[15] Recently, PD-1 has been identified as a marker of exhausted T cells in chronic infectious disease.[16–22] Among the numerous mechanisms of tumor-induced immunosuppression by which tumors can escape from immune surveillance, a number of studies have suggested a role of the interaction between PD-1 and the programmed death-ligand 1 (PD-L1) in inhibiting the effector functions of antigen-specific $CD8^+$ T cells.[23–26] PD-1 is expressed on tumor-infiltrating $CD8^+$ T cells in tumors or on antigen-specific CD8 T cells in hosts with tumors, and the function of these PD-1^+ T cells is impaired.[27,28] PD-L1 is expressed at high levels in several different cancers,[29] and the high levels of expression of PD-L1 on tumors is strongly associated with poor prognosis.[30,31] A recent study showed that the blockade of PD-1–PD-L signaling restored functional T-cell responses in several cancers and, subsequently, improved clinical outcomes.[32–34]

In this study, the antitumor effects of the combination of IFN-α-transfected tumor cell vaccine therapy and PD-1 blockade were evaluated in a poorly immunogenic murine colorectal cancer

[1]Division of Gastroenterology, Department of Medicine, Showa University School of Medicine, Shinagawa-ku, Tokyo, Japan and [2]Promotion Center of Pharmaceutical Education, Showa University School of Pharmacy, Shinagawa-ku, Tokyo, Japan. Correspondence: Dr J Eguchi, Division of Gastroenterology, Department of Medicine, Showa University School of Medicine, 1-5-8 Hatanodai, Shinagawa-ku, Tokyo 142-8666, Japan.
E-mail: j.eguchi@med.showa-u.ac.jp
Received 13 December 2011; revised 30 May 2012; accepted 31 May 2012; published online 13 July 2012

system as a preliminary investigation of the combined therapy before clinical studies. We show that, when parental tumor-bearing mice were injected with IFN-α-overexpressing tumor cells and anti-PD-1 blocking antibody, the outgrowth of the established parental tumors was significantly suppressed. Furthermore, in order to explore the mechanisms of the antitumor effects induced by IFN-α and anti-PD-1 combination therapy, we performed immunohistologic staining of the tumors and tried to induce tumor-specific T lymphocytes.

MATERIALS AND METHODS

Mice

Female 6-week-old C57BL/6 (B6) mice were purchased from Sankyo Lab Service (Tokyo, Japan) for use in experiments from 8 to 12 weeks of age. Mice were maintained in an animal care facility at Showa University. This study was approved by the ethical committee for Animal Experiments of Showa University (permission #2011-1111).

Cell lines, culture medium and reagents

The MC38 murine colorectal adenocarcinoma cell line, the MCA205 fibrosarcoma cell line (both B6 mouse origin) and yeast artificial chromosome-1 (YAC-1) lymphoma cells were maintained in RPMI-1640 medium supplemented with 10% heat-inactivated fetal calf serum, 2 mM L-glutamine, 100 IU ml^{-1} penicillin, 100 μg ml^{-1} streptomycin, 10 mM HEPES buffer, 1 mM minimum essential medium sodium pyruvate and 0.1 mM minimum essential medium nonessential amino acids (complete medium) in a humidified incubator with 5% CO_2 in air at 37 °C. All cell culture reagents were purchased from Life Technologies (Gaithersburg, MD). YAC-1 cells were used as target cells in order to assess the nonspecific killing in cytolytic assays.

The MC38 cell line was genetically modified in order to produce murine IFN-α (MC38-IFNα), as described previously.[35] The expression of IFN-α was confirmed by enzyme-linked immunosorbent assay (ELISA) using a commercially available kit according to the manufacturer's instructions (mouse IFN-α ELISA, PBL InterferonSource, New Brunswick, NJ). MC38 cells expressing the neomycin-resistance gene following retroviral transduction with MFG-Neo (MC38-Neo) were used as control cells.[35] Gamma-irradiation (100 Gy for tumor cells) was performed with Gammacell 3000 Elan (Nordion, Kanata, ON, Canada). As reported previously, 1×10^5 cells of MC38-IFNα produce IFN-α 20.8 ± 0.5 ng/48 h, and MC38-wild type (WT) cells do not produce any IFN-α. IFN-α gene transduction does not affect the growth of tumor cells *in vitro* or the survival of γ-irradiated tumor cells.[36]

In vitro culture of splenocytes from immunized mice stimulated with a genetically modified MC38 or anti-PD-1 antibody

Mice were initially inoculated with 1×10^5 MC38-IFNα tumor cells on days 0, 7 and 14. Subsequently, MC38-immune mice received challenges of 3×10^5 MC38-WT cells on day 28. Splenocytes (3×10^6 cells ml^{-1}) were harvested from these mice on day 35 and then incubated in the presence of irradiated (100 Gy) and genetically modified MC38 (2×10^5 cells ml^{-1}) or 10 μg ml^{-1} of anti-PD-1 antagonistic antibody (BioLegend, San Diego, CA) either alone or in combination in complete medium. Cells were harvested every 3 days, and cell numbers were determined microscopically. IFN-γ and IL-10 production of splenocytes from immunized mice were observed. After 3 days of incubation, IFN-γ and IL-10 concentrations in the culture supernatant were measured by ELISA using a commercially available kit according to the manufacturer's instructions (mouse IFN-γ ELISA and mouse IL-10 ELISA, R&D Systems, Minneapolis, MN).

Flow cytometric analyses of lymphocytes from immunized mice stimulated with a genetically modified MC38 or anti-PD-1 antibody

In order to observe the immunogenic effects of IFN-α and anti-PD-1 antibody, flow cytometric analyses was performed using FACSCalibur (Nippon Becton Dickinson, Tokyo, Japan). After 7 days of *in vitro* incubation, splenocytes from MC38-IFNα immunized mice were harvested. $CD4^+$ and $CD8^+$ T cells were separated from splenocytes using CD4 and CD8 microbeads (MACS system; Miltenyi Biotec, Bergisch Gladbach, Germany), and isolated using an autoMACS Pro Separator (Miltenyi Biotec). These cells were stained with fluorescein isothiocyanate-conjugated and phycoerythrin-conjugated monoclonal antibodies. The monoclonal antibodies used in this assay were anti-H-$2K^b$, CD4, CD8, CD25, 7-AAD (obtained from Nippon Becton Dickinson) and caspase-8 (Medical and Biological Laboratories, Nagoya, Japan) antibodies.

Therapeutic models

In order to evaluate the potential to treat established tumors, we measured the size of established WT tumors of mice treated with genetically modified MC38 cells and antibody, as previously described.[35] In brief, B6 mice were injected subcutaneously with 1×10^5 MC38-WT cells in the right flank. In all, 7, 10 and 14 days after the WT inoculation, treatment was performed following the injection of 1×10^5 genetically modified MC38 or 200 μg of anti-PD-1 antibody either alone or in combination into the contralateral (left) flank. Each experiment involved six mice per group. Tumor size was measured twice a week using vernier calipers. Experiments with the therapeutic model were performed three times.

In vivo antibody-mediated depletion of leukocytes

To determine the role of the immune system in reduction of tumor growth *in vivo*, $CD4^+$ T cells, $CD8^+$ T cells or NK cells were depleted as reported previously.[13] Culture medium of hybridomas producing the following antibodies was used at appropriate dilutions/concentrations: anti-CD4 (GK1.5, TIB207; American Type Culture Collection (ATCC), Manassas, VA), anti-CD8 (2.43, TIB210; ATCC) and anti-asialo-GM1 (anti-NK cells; WAKO, Osaka, Japan). All antibody doses and treatment regimens have been identified for the same batch of antibodies used in preliminary studies. Mice were inoculated with 1×10^5 cells of MC38-WT 3 days after depletion of leukocytes, and MC38-IFNα and anti-PD-1 antibody combination treatment were performed 7, 10 and 14 days after the WT inoculation. This treatment was confirmed to completely delete the desired cell population for the entire duration of the study, as determined by flow cytometric analysis (data not shown).

Immunohistologic analysis

B6 mice were injected subcutaneously in the right flank with 1×10^5 MC38-WT cells. On days 7, 10 and 14, 1×10^5 MC38-IFNα and/or 200 μg of anti-PD-1 antagonistic antibody were inoculated into the contralateral (left) flank. Tumor tissues were harvested 4 days after the last inoculation (18 days after WT inoculation) and were immediately embedded in optimal cutting temperature compound (Tissue-Tek, Elkhart, IN) and frozen. Serial 5-μm sections were exposed to anti-CD4, anti-CD8a, anti-CD11c and anti-Gr-1 antibodies (Nippon Becton Dickinson) and anti-PDL1-antibody (BioLegend). Rat IgG2a (Nippon Becton Dickinson) was used as a control antibody. Immunostaining was completed with a Vectastain ABC kit (Vector Laboratories, Burlingame, CA). Immunoreactive cells were visualized using light microscopy (400 ×) and counted in 10 fields in a blinded fashion. Each experiment involved two mice per group.

Induction of tumor-specific CTL

Mice were initially inoculated with 1×10^5 MC38-IFNα tumor cells and/or 200 μg of anti-PD-1 antibody on days 0, 7 and 14. Subsequently, MC38-immune mice received challenges of 3×10^5 MC38-WT cells on day 28. Splenocytes (3×10^6 cells ml^{-1}) were harvested from these mice on day 42 and then stimulated *in vitro* with irradiated (100 Gy) MC38-IFNα tumor cells (3×10^5 cells ml^{-1}). Seven days later, responder cells (1×10^6 cells ml^{-1}) were restimulated with irradiated MC38-IFNα tumor cells (100 Gy, 1×10^5 cells ml^{-1}) and syngeneic dendritic cells (2×10^5 cells ml^{-1}) in the presence of 50 IU ml^{-1} of recombinant mouse IL-2 (R&D Systems). Dendritic cells were generated from bone marrow cells of B6 mice using murine granulocyte-macrophage colony-stimulating factor (10 ng ml^{-1}) and IL-4 (10 ng ml^{-1}) that was obtained from PeproTech EC (London, England), as

reported previously.[36] Cytolytic assays were performed 7 days after the last stimulation using the responder cells as effector cells.

Cytolytic assays

Tumor-stimulated effector cells were assessed for cytolytic activity against MC38-WT, MCA205 and YAC-1 cells in triplicate in a 4-h ^{51}Cr-release assay. Target cells (1×10^6 cells ml^{-1}) were labeled with 3.7 MBq of $Na_2{}^{51}CrO_4$ (GE Healthcare, Tokyo, Japan) for 1 h at 37 °C. Labeled cells were washed and resuspended. Target cells (5×10^3) and various numbers of effector cells at the indicated effector to target ratios (E:T) were plated in 200 μl of complete medium in each well of the 96-well round-bottom plates. ^{51}Cr-release was measured after a 4-h incubation at 37 °C. The percent lysis was determined using the formula (release in assay−spontaneous release) × 100/(maximum release−spontaneous release). Maximum release was determined by the lysis of labeled target cells with 1% Triton X-100. Spontaneous release was measured by incubating target cells in the absence of effector cells and was <15% of maximum release.

Statistical analyses

Statistical analyses were carried out using means s.d., one-way analysis of variance and Turkey's honestly significant difference *post-hoc* test. Differences between groups were considered significant when the P values were <0.05.

RESULTS

Anti-PD-1 antibody and IFN-α-overexpressing cells enhanced IFN-γ production and reduced IL-10 production by splenocytes from mice immunized with MC38-IFNα

First, we observed the *in vitro* effects of MC38-IFNα and the anti-PD-1 antibody. Mice were initially inoculated with MC38-IFNα three times. Subsequently, these mice received challenges of MC38-WT cells 14 days after the last immunization. One week later, splenocytes of the treated mice were harvested and stimulated with the MC38-IFNα or anti-PD-1 antibody *in vitro*. After 3 days of incubation, the IFN-γ and IL-10 concentrations of

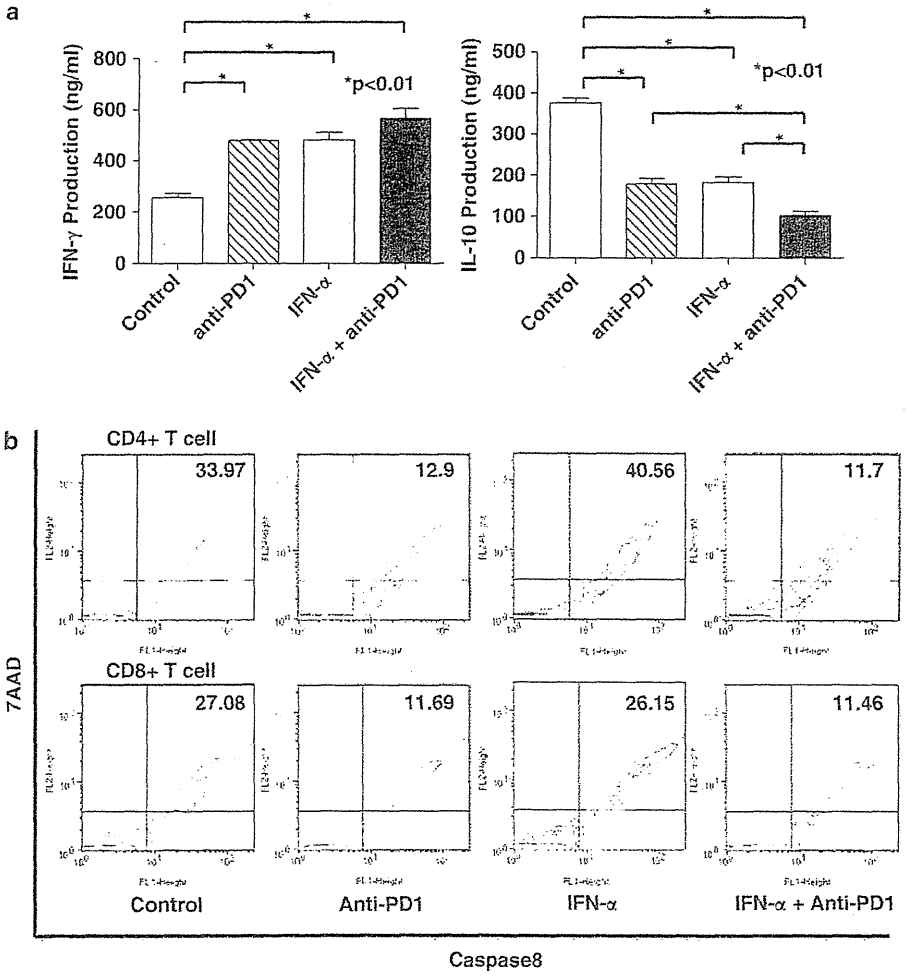

Figure 1. (**a**) The combination of interferon (IFN)-α and anti-programmed cell death-1 (PD-1) enhances IFN-γ production but reduces the interleukin (IL)-10 production of splenocytes obtained from mice immunized with MC38-IFNα after *in vitro* stimulation. Mice were inoculated with MC38-IFNα cells three times and then injected with MC38-wild-type (WT) cells 2 weeks after the last MC38-IFNα inoculation. Seven days later, mice were killed, and splenocytes from these mice were stimulated *in vitro* with MC38-IFNα cells alone or in combination with an anti-PD-1 antibody. After 3 days of incubation, IFN-γ and IL-10 concentrations in the culture supernatant were measured by an enzyme-linked immunosorbent assay (ELISA). (**b**) Blockade of PD-1 reduced the level of apoptosis in lymphocytes from mice immunized with MC38-IFNα. Splenocytes from mice immunized with MC38-IFNα were stimulated with MC38-IFNα or anti-PD-1 antibody. After 7 days of incubation, splenocytes were isolated to CD4$^+$ and CD8$^+$ T cells and stained with the phycoerythrin (PE)-conjugated anti-7AAD and fluorescein isothiocyanate (FITC)-conjugated anti-caspase-8. Numbers in each histogram indicate the percentage of 7AAD$^+$/caspase-8$^+$ cells in the total CD4$^+$ or CD8$^+$ population. These experiments were repeated three times, and a representative result is shown.

Table 1. Flow cytometric analyses of lymphocytes from immunized mice stimulated with a genetically modified MC38 or anti-PD-1 antibody

Treatment	*Caspase-8(−)/ 7AAD(−)*	*Caspase-8(+)/ 7AAD(−)*	*Caspase-8(+)/ 7AAD(+)*
CD4			
Control	55.29	10.74	33.97
Anti-PD-1	74.25	12.85	12.9
IFN-α	47.72	11.72	40.56
IFNα+anti-PD-1	80.12	8.13	11.7
CD8			
Control	68.32	4.14	27.08
Anti-PD-1	85.66	2.61	11.69
IFN-α	71.32	2.37	26.15
IFNα+anti-PD-1	86.35	2.16	11.46

Abbreviations: IFN, interferon; PD-1, programmed cell death-1.
Numbers indicate the percentage of positive cells in the total $CD4^+$ or $CD8^+$ population.

the supernatant of each culture were measured by ELISA. IFN-γ production was clearly increased in the IFN-α and anti-PD-1 antibody-stimulated group compared with controls (IFN + anti-PD-1 vs control, $P = 0.009$; Figure 1a), whereas IL-10 production was suppressed significantly ($P < 0.001$, Figure 1a). In addition, the proliferation rate of the splenocytes did not differ significantly between the control group and the treatment groups (data not shown). These results suggest that IFN-α and anti-PD-1 elicited a potent Th1-type response.

PD-1 blockade prevented the apoptosis of lymphocytes from mice immunized with MC38-IFNα

To determine the immunogenic effects of IFN-α and PD-1 blockade, flow cytometric analyses was performed. Splenocytes from mice immunized with MC38-IFNα were stimulated with MC38-IFNα or anti-PD-1 antibody. After 7 days of incubation, splenocytes were isolated to $CD4^+$ and $CD8^+$ T cells and analyzed by flow cytometry. Treatment with anti-PD-1 antibody decreased the population of caspase-8^+ $7AAD^+$ T-cell subsets (Table 1 and Figure 1b). This result indicate that blockade of PD-1 reduced the level of apoptosis in both $CD4^+$ and $CD8^+$ T cell. Furthermore, there was no significant difference on percentage of $CD4^+$ regulatory T cells in every group (data not shown).

Therapeutic inoculations with the combination of IFN-α-transduced MC38 tumor cells and the anti-PD-1 antibody suppressed the *in vivo* growth of established MC38 tumors

We examined the therapeutic effects of MC38-IFNα and the anti-PD-1 antibody. Mice bearing established WT MC38 tumors were treated with an injection of MC38-IFNα alone, anti-PD-1 antibody alone or the combination. Starting 7 days after the inoculation of MC38-WT, mice were injected every 3 days with the MC38-IFNα cells and/or the anti-PD-1 antibody in the opposite flank. A significant suppression of outgrowth of the established tumors was observed in the IFN-α and anti-PD-1 combination treatment group (IFN + anti-PD-1, $174.17 \pm 35.54\,mm^2$ vs control, $328.67 \pm 26.36\,mm^2$ on day 28, $P = 0.020$ vs controls; Figure 2a). Although the mean tumor size of the mice was relatively suppressed compared with the control group, the suppressive effects on the established tumors were not significant when the immunizations were performed with MC38-IFNα alone (IFN, $220.17 \pm 36.70\,mm^2$ vs control, $328.67 \pm 26.36\,mm^2$ on day 28, $P = 0.121$ vs controls) or with the anti-PD-1-antibody alone (anti-PD-1, $277.00 \pm 31.53\,mm^2$ vs control, $328.67 \pm 26.36\,mm^2$ on day 28, $P = 0.636$ vs controls).

$CD4^+$ and $CD8^+$ cells are responsible for antitumor effects induced by combination of IFN-α-transduced MC38 tumor cells and the anti-PD-1 antibody

To characterize immune mechanisms suppressing *in vivo* tumor growth in the therapeutic model, immunocompetent B6 mice were depleted of $CD4^+$ T cells, $CD8^+$ T cells or asialo-$GM1^+$ cells using specific antibodies. Depletion of $CD4^+$ T cells and $CD8^+$ T cells abrogated therapeutic effect induced by MC38-IFNα and anti-PD-1 antibody combination treatment (Figure 2b). On the other hand, depletion of NK cells did not affect to the tumor suppression. These results suggest that both $CD4^+$ and $CD8^+$ T cells are responsible for antitumor response in mice treated with IFN-α and anti-PD-1.

Combined MC38-IFNα and anti-PD-1 antibody treatment induced the infiltration of CD4- and CD8-positive cells in established WT tumors

In order to analyze the antitumor mechanisms that were induced by the combined IFN-α and anti-PD-1 therapy, we performed immunohistochemical staining using the WT tumor tissues of the treated mice. The results showed that marked infiltration of both $CD4^+$ cells and $CD8^+$ cells had occurred by the addition of the anti-PD-1 antibody compared with controls and the group treated with MC38-IFNα alone (Table 2 and Figure 3). In addition, only a few $CD11c^+$ and $Gr\text{-}1^+$ cells could be detected in the WT tumors of every group. These results suggest that the antitumor effects of the IFN-α and anti-PD-1 therapy were dependent on both $CD4^+$ cells and $CD8^+$ cells.

Marked tumor-specific cytolysis was detected when splenocytes from mice treated with both MC38-IFNα and the anti-PD-1 antibody were used as effector cells

Mice were initially inoculated with MC38-IFNα and/or the anti-PD-1 antibody on days 0, 7 and 14. Subsequently, these mice received challenges of MC38-WT cells on day 28. Splenocytes of the treated mice were harvested on day 35 and stimulated weekly *in vitro* with the MC38-IFNα cells twice. Cytolytic assays against the MC38 or the YAC-1 cells, which are sensitive to NK cells, were performed 7 days after the second stimulation. A high specificity for MC38 was observed when treatment was performed with MC38-IFNα alone ($32.5 \pm 7.2\%$ for MC38 and $10.3 \pm 2.6\%$ for YAC-1, E:T = 20, $P = 0.012$; Figure 4a) or the combination of both MC38-IFNα and the anti-PD-1-antibody ($58.1 \pm 6.7\%$ for MC38 and $14.1 \pm 1.7\%$ for YAC-1, E:T = 20, $P < 0.001$). When splenocytes from mice that were treated with only the anti-PD-1 antibody were used as effector cells, comparable cytolysis was detected for both targets of MC38 and YAC-1 cells ($18.6 \pm 5.9\%$ for MC38 and $18.2 \pm 2.7\%$ for YAC-1, E:T = 20, $P = 0.231$). Compared with the IFN-α or anti-PD-1 single treatment groups, significant cytotoxicity against MC38 was observed in the IFN-α and anti-PD-1 combination treatment group ($P < 0.001$ vs anti-PD-1, $P = 0.002$ vs MC38-IFNα; Figure 4b). These findings suggest that anti-PD-1 has a minimal ability to induce tumor-specific cytotoxicity, but it can enhance the strong specific response that is induced by IFN-α.

DISCUSSION

Gene therapy using tumor cells that are genetically modified to produce cytokines has been studied in several therapeutic models. We have previously reported that the combination of IFN-α gene-transduced tumor-based vaccination therapy and IL-4 or IL-12 gene therapy suppresses the outgrowth of established tumors.[13,14] Although the suppressive effects of established tumors were observed in these cytokine combination therapy models, we

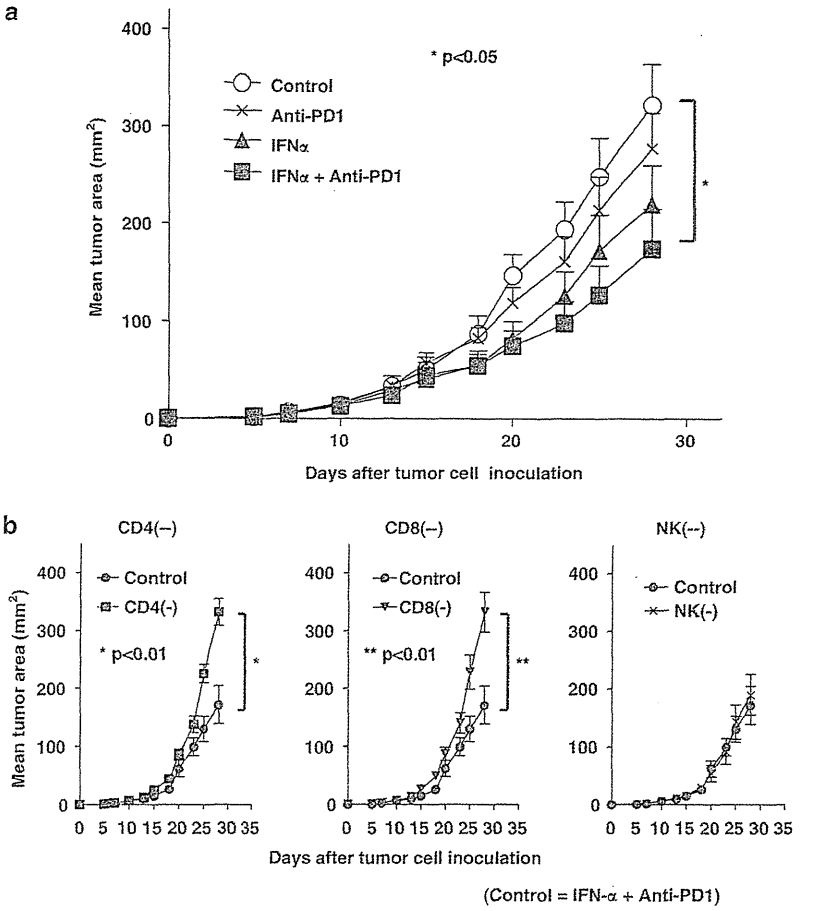

Figure 2. (**a**) Therapeutic inoculations with the combination of interferon (IFN)-α-transduced MC38 tumor cells and the anti-programmed cell death-1 (PD-1) antibody suppress the *in vivo* growth of established MC38 tumors. Animals were inoculated with MC38-wild type (WT) in the flank on day 0. Established MC38 cells were treated three times with MC38-IFNα alone, anti-PD-1 antibody alone or the combination in the contralateral flank every third day starting 7 days after WT tumor injection. (**b**) $CD4^+$ and $CD8^+$ cells are responsible for antitumor effects induced by combination of IFN-α and anti-PD-1. Mice were depleted of $CD4^+$ T cells, $CD8^+$ T cells or asialo-$GM1^+$ cells using specific antibodies 3 days before the WT tumor inoculation. MC38-IFNα and anti-PD-1 antibody combination therapy was performed every third day starting 7 days after WT tumor injection. Six mice were studied in each group. The results are reported as mean tumor area (mm^2) ± s.e. Significance at the 95% confidence limits is indicated. This experiment was performed twice with similar results.

Table 2. Immunohistologic analysis of $CD8^+$ T-cell infiltration in the established wild-type tumors treated with MC38-IFN-α and/or anti-PD-1 antagonistic antibody

Treatment	*Number of positive cells*			
	$CD4^+$ cells	*$CD8^+$cells*	*$CD11c^+$ cells*	*$Gr\text{-}1^+$ cells*
Control	3.6 ± 3.6	7.8 ± 6.1	3.3 ± 1.9	4.6 ± 9.0
Anti-PD-1	58.4 ± 55.4	33.8 ± 45.6	1.7 ± 1.8	0.8 ± 1.2
IFN-α	11.8 ± 6.4	15.0 ± 10.2	0.5 ± 1.2	0.8 ± 0.4
IFN-α+anti-PD-1	60.0 ± 44.8	33.2 ± 7.1	5.5 ± 5.8	2.5 ± 3.5

Abbreviations: IFN, interferon; PD-1, programmed cell death-1.
Immunoreactive cells were counted in five microscopic fields (400 ×) without knowledge of the experimental group. Results are reported as mean number of positive cells ± s.d.

did not see reductions in the size of all of the parental tumors. Therefore, further improvements in the treatment are needed before clinical application. In addition, we focused on PD-1, which has been identified as a marker of exhausted T cells.[16–22] As a blockade of PD-1 signaling has been shown to improve clinical outcome and restore functional T-cell responses in cancers,[32–34] we hypothesized that the PD-1 blockade had potential to enhance the Th1 responses elicited by the IFN-α gene-transduced tumor-based vaccination therapy. In this study, we investigated the antitumor effects and mechanisms of the combination of the IFN-α-transduced tumor cell vaccine therapy and PD-1 blockade.

First, we examined the *in vitro* effects of the IFN-α-transduced tumor cells and the anti-PD-1 antibody in a culture medium of splenocytes. Both IFN-α and the blockade of PD-1 obviously increased IFN-γ production and suppressed IL-10 production, and additive effects were observed with the combination of IFN-α and anti-PD-1. These results suggest that IFN-α and anti-PD-1 promoted Th1-type antitumor immune responses, and the responses were enhanced in cooperation with each other. From these results of the *in vitro* additive antitumor effects, we tried to treat tumor-bearing mice with the IFN-α and anti-PD-1 antibody, and a significant suppression of the outgrowth of the established tumors was observed only in the combination treatment group. The IFN-α or anti-PD-1 single therapy groups showed a weak, but not significant suppression of the established tumors compared with the control group. Leukocyte depletion

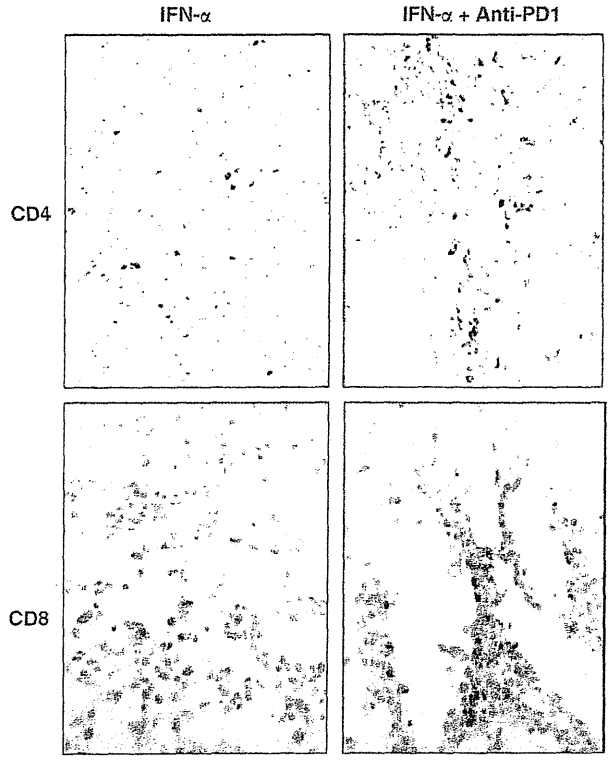

Figure 3. $CD4^+$ and $CD8^+$ cells markedly infiltrated into the established wild-type (WT) tumors of mice inoculated with the combination of MC38-interferon (IFN)-α cells and anti-programmed cell death-1 (PD-1) antibody. B6 mice were injected subcutaneously three times with MC38-IFNα cells and anti-PD-1-antibody either alone or in combination into the contralateral flank of the established WT tumor. Tumor tissues were harvested 4 days after therapeutic inoculation and stained with anti-CD4 and anti-CD8 antibodies. Immunoreactive cells were observed using light microscopy (400 x).

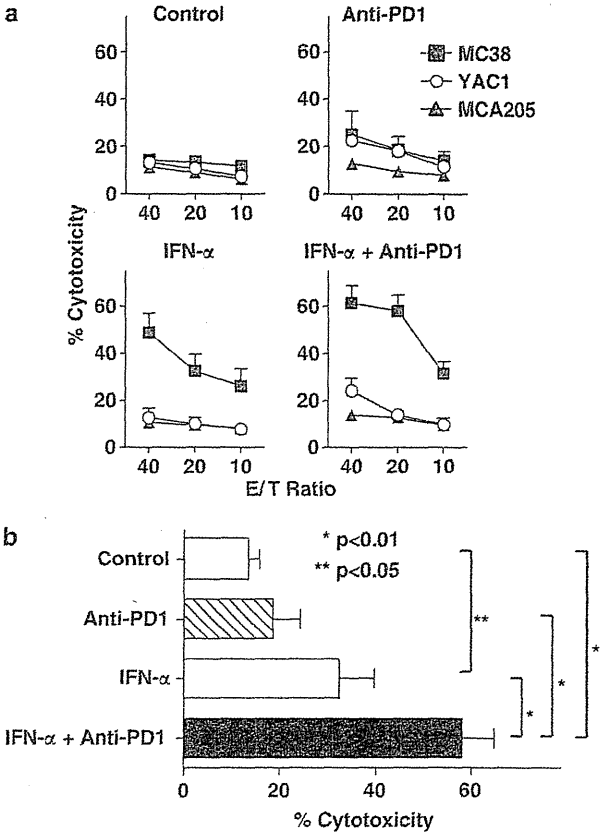

Figure 4. The combination treatment with interferon (IFN)-α and anti- programmed cell death-1 (PD-1) antibody induces potent tumor-specific cytolysis. (**a**) Mice were initially inoculated with MC38-IFNα cells and/or anti-PD-1 antibody on days 0, 7 and 14. Subsequently, MC38-immune mice received challenges of MC38-wild-type (WT) cells on day 28. Splenocytes were harvested from these mice on day 42 and then stimulated *in vitro* with MC38-IFNα cells and syngeneic dendritic cells twice weekly. The cytolytic assay against MC38, MCA205 or yeast artificial chromosome-1 (YAC-1) cells was performed 7 days after the last stimulation. Results are reported as mean percent cytotoxicity + s.d. This experiment was performed twice with similar results. (**b**) The cytolytic assay against MC38 was performed on an effector to target ratio of 20. E:T, effector to target.

experiments demonstrated that both $CD4^+$ T cells and $CD8^+$ T cells were essential to the tumor suppression induced by combination therapy. In contrast, the depletion of NK cell did not affect to the therapeutic effect in this model.

Immunohistologic analyses of the established tumors in the mice that were treated with anti-PD-1 showed marked infiltration of both $CD4^+$ cells and $CD8^+$ cells compared with controls and the group treated with MC38-IFNα alone. These data support the results of a previous study that showed that blockade of PD-1 signaling pathways reversed T-cell exhaustion and restored antitumor immunity.[34] Interestingly, the proliferation rate of splenocytes did not differ significantly between the control group and the anti-PD-1 treatment groups in the *in vitro* culture setting (data not shown). The conditions and microenvironment of the local tumor sites seemed to lead to this discrepancy between the *in vitro* and *in vivo* results because immunohistochemical staining confirmed that established MC38-WT tumors expressed abundant PD-L1 molecules (data not shown). However, we demonstrated that blockade of PD-1 reduced the level of apoptosis in lymphocytes on *in vitro* setting. These observations suggest that the PD-1 blockade prevented the apoptosis of lymphocytes and maintained the survival and infiltration of tumor-specific T cells in the local tumor environment, which strongly expressed PD-L1 molecules.

Although the PD-1 blockade recruited lymphocytes to the tumor sites, the therapeutic effects were not remarkable for the treatment with anti-PD-1 alone. In order to assess this result, we tried to induce tumor-specific CTLs from the splenocytes of IFN-α or anti-PD-1-treated mice and then perform cytolytic assays. A high specificity for MC38 was observed when treatment was performed with IFN-α, whereas only nonspecific cytolysis was detected with the anti-PD-1 treatment. Furthermore, specific cytolysis against MC38 was observed more potently with the combined IFN-α and anti-PD-1 treatment group compared with the IFN-α single treatment group. These observations suggest that IFN-α elicited tumor-specific CTLs, whereas the blockade of PD-1 mainly maintained the specific response induced by IFN-α, preventing CTLs from apoptosis. Thus, the combined therapy is considered to be reasonable because both IFN-α and the blockade of PD-1 revealed antitumor effects by different mechanisms. Also recent study show similar results and support our study that blockade of PD-1 can enhance the immune response stimulated by cytokine therapy in murine colon cancer model.[37]

The clinical use of this kind of tumor-based gene therapy may be limited because of the need to transduce genes in patients' tumor cells. IFN-α gene-transduced cells were used in this study, although the establishment of transduced cells, which produce a

high amount of IFN-α, would be difficult in the clinical setting. Administering recombinant IFN-α repetitively seems to be simple, but there was no therapeutic effect observed in our past study (data not published). In order to facilitate this, the method of cytokine gene delivery will need to be modified. In addition, it is not established whether anti-PD-1 therapy is effective against the tumors, which are negative for the expression of PD-L1. In order to resolve these problems, we are now planning to use other tumor cell lines and reevaluate the antitumor effects of the PD-1 blockade on the established tumors.

In conclusion, our findings suggest that the combination of IFN-α immunotherapy and PD-1 blockade therapy has potential for inducing potent immune responses and that this might be considered as a possible candidate for clinical trials of cancer vaccines, although further investigations are required.

CONFLICT OF INTEREST

The authors declare no conflict of interest.

ACKNOWLEDGEMENTS

We thank Ms Tomoe Shimazaki and Ms Hisako Nozawa for technical assistance. This study was supported in part by a Grant-in-Aid for Young Scientists (B) from the Ministry of Education, Culture, Sports, Science and Technology of Japan for JE; a Grant-in-Aid for Scientific Research (C) from the Ministry of Education, Culture, Sports, Science and Technology of Japan; and a grant from the Ministry of Health, Labor, and Welfare of Japan for KH.

REFERENCES

1 O'Connell J, Bennett MW, O'Sullivan GC, Collins JK, Shanahan F. The Fas counterattack: cancer as a site of immune privilege. *Immunol Today* 1999; **20**: 46–52.
2 Bronte V, Serafini P, Apolloni E, Zanovello P. Tumor-induced immune dysfunctions caused by myeloid suppressor cells. *J Immunother* 2001; **24**: 431–446.
3 Chen L, Linsley PS, Hellstrom KE. Costimulation of T cells for tumor immunity. *Immunol Today* 1993; **14**: 483–486.
4 Colombo MP, Forni G. Cytokine gene transfer in tumor inhibition and tumor therapy: where are we now? *Immunol Today* 1994; **15**: 48–51.
5 Musiani P, Modesti A, Giovarelli M, Cavallo F, Colombo MP, Lollini PL *et al.* Cytokines, tumour-cell death and immunogenicity: a question of choice. *Immunol Today* 1997; **18**: 32–36.
6 Eguchi J, Kuwashima N, Hatano M, Nishimura F, Dusak JE, Storkus WJ *et al.* IL-4-transfected tumor cell vaccines activate tumor-infiltrating dendritic cells and promote type-1 immunity. *J Immunol* 2005; **174**: 7194–7201.
7 Juang Y, Lowther W, Kellum M, Au WC, Lin R, Hiscott J *et al.* Primary activation of interferon A and interferon B gene transcription by interferon regulatory factor 3. *Proc Natl Acad Sci USA* 1998; **95**: 9837–9842.
8 Marie I, Durbin JE, Levy DE. Differential viral induction of distinct interferon-alpha genes by positive feedback through interferon regulatory factor-7. *EMBO J* 1998; **17**: 6660–6669.
9 Okada H, Villa L, Attanucci J, Erff M, Fellows WK, Lotze MT *et al.* Cytokine gene therapy of gliomas: effective induction of therapeutic immunity to intracranial tumors by peripheral immunization with interleukin-4 transduced glioma cells. *Gene Ther* 2001; **8**: 1157–1166.
10 Belardelli F. Role of interferons and other cytokines in the regulation of the immune response. *APMIS* 1995; **103**: 161–179.
11 von Hoegen P, Zawatzky R, Schirrmacher V. Modification of tumor cells by a low dose of Newcastle disease virus. III Potentiation of tumor-specific cytolytic T cell activity via induction of interferon-alpha/beta. *Cell Immunol* 1990; **126**: 80–90.
12 Hiroishi K, Tuting T, Lotze MT. IFN-alpha-expressing tumor cells enhance generation and promote survival of tumor-specific CTLs. *J Immunol* 2000; **164**: 567–572.
13 Eguchi J, Hiroishi K, Ishii S, Mitamura K. Interferon-alpha and interleukin-12 gene therapy of cancer; interferon-alpha induces tumor-specific immune responses while interleukin-12 stimulates non-specific killing. *Cancer Immunol Immunother* 2003; **52**: 378–386.
14 Eguchi J, Hiroishi K, Ishii S, Baba T, Matsumura T, Hiraide A *et al.* Interleukin-4 gene transduced tumor cells promote a potent tumor-specific Th1-type response in cooperation with interferon-alpha transduction. *Gene Ther* 2005; **12**: 733–741.
15 Ishida Y, Agata Y, Shibahara K, Honjo T. Induced expression of PD-1, a novel member of the immunoglobulin gene superfamily, upon programmed cell death. *EMBO J* 1992; **11**: 3887–3895.
16 Day CL, Kaufmann DE, Kiepiela P, Brown JA, Moodley ES, Reddy S *et al.* PD-1 expression on HIV-specific T cells is associated with T-cell exhaustion and disease progression. *Nature* 2006; **443**: 350–354.
17 Petrovas C, Casazza JP, Brenchley JM, Price DA, Gostick E, Adams WC *et al.* PD-1 is a regulator of virus-specific CD8+ T cell survival in HIV infection. *J Exp Med* 2006; **203**: 2281–2292.
18 Trautmann L, Janbazian L, Chomont N, Said EA, Gimmig S, Bessette B *et al.* Upregulation of PD-1 expression on HIV-specific CD8+ T cells leads to reversible immune dysfunction. *Nat Med* 2006; **12**: 1198–1202.
19 Urbani S, Amadei B, Tola D, Massari M, Schivazappa S, Missale G *et al.* PD-1 expression in acute hepatitis C virus (HCV) infection is associated with HCV-specific CD8 exhaustion. *J Virol* 2006; **80**: 11398–11403.
20 Penna A, Pilli M, Zerbini A, Orlandini A, Mezzadri S, Sacchelli L *et al.* Dysfunction and functional restoration of HCV-specific CD8 responses in chronic hepatitis C virus infection. *Hepatology* 2007; **45**: 588–601.
21 Boettler T, Panther E, Bengsch B, Nazarova N, Spangenberg HC, Blum HE *et al.* Expression of the interleukin-7 receptor alpha chain (CD127) on virus-specific CD8+ T cells identifies functionally and phenotypically defined memory T cells during acute resolving hepatitis B virus infection. *J Virol* 2006; **80**: 3532–3540.
22 Boni C, Fisicaro P, Valdatta C, Amadei B, Di Vincenzo P, Giuberti T *et al.* Characterization of hepatitis B virus (HBV)-specific T-cell dysfunction in chronic HBV infection. *J Virol* 2007; **81**: 4215–4225.
23 Blank C, Kuball J, Voelkl S, Wiendl H, Becker B, Walter B *et al.* Blockade of PD-L1 (B7-H1) augments human tumor-specific T cell responses *in vitro*. *Int J Cancer* 2006; **119**: 317–327.
24 Fourcade J, Kudela P, Sun Z, Shen H, Land SR, Lenzner D *et al.* PD-1 is a regulator of NY-ESO-1-specific CD8+ T cell expansion in melanoma patients. *J Immunol* 2009; **182**: 5240–5249.
25 Iwai Y, Ishida M, Tanaka Y, Okazaki T, Honjo T, Minato N. Involvement of PD-L1 on tumor cells in the escape from host immune system and tumor immunotherapy by PD-L1 blockade. *Proc Natl Acad Sci USA* 2002; **99**: 12293–12297.
26 Blank C, Brown I, Peterson AC, Spiotto M, Iwai Y, Honjo T *et al.* PD-L1/B7H-1 inhibits the effector phase of tumor rejection by T cell receptor (TCR) transgenic CD8+ T cells. *Cancer Res* 2004; **64**: 1140–1145.
27 Ahmadzadeh M, Johnson LA, Heemskerk B, Wunderlich JR, Dudley ME, White DE *et al.* Tumor antigen-specific CD8 T cells infiltrating the tumor express high levels of PD-1 and are functionally impaired. *Blood* 2009; **114**: 1537–1544.
28 Gehring AJ, Ho ZZ, Tan AT, Aung MO, Lee KH, Tan KC *et al.* Profile of tumor antigen-specific CD8 T cells in patients with hepatitis B virus-related hepatocellular carcinoma. *Gastroenterology* 2009; **137**: 682–690.
29 Dong H, Strome SE, Salomao DR, Tamura H, Hirano F, Flies DB *et al.* Tumor-associated B7-H1 promotes T-cell apoptosis: a potential mechanism of immune evasion. *Nat Med* 2002; **8**: 793–800.
30 Gao Q, Wang XY, Qiu SJ, Yamato I, Sho M, Nakajima Y *et al.* Overexpression of PD-L1 significantly associates with tumor aggressiveness and postoperative recurrence in human hepatocellular carcinoma. *Clin Cancer Res* 2009; **15**: 971–979.
31 Thompson RH, Dong H, Lohse CM, Leibovich BC, Blute ML, Cheville JC *et al.* PD-1 is expressed by tumor-infiltrating immune cells and is associated with poor outcome for patients with renal cell carcinoma. *Clin Cancer Res* 2007; **13**: 1757–1761.
32 Zhang L, Gajewski TF, Kline J. PD-1/PD-L1 interactions inhibit antitumor immune responses in a murine acute myeloid leukemia model. *Blood* 2009; **114**: 1545–1552.
33 Mumprecht S, Schurch C, Schwaller J, Solenthaler M, Ochsenbein AF. Programmed death 1 signaling on chronic myeloid leukemia-specific T cells results in T-cell exhaustion and disease progression. *Blood* 2009; **114**: 1528–1536.
34 Sakuishi K, Apetoh L, Sullivan JM, Blazar BR, Kuchroo VK, Anderson AC. Targeting Tim-3 and PD-1 pathways to reverse T cell exhaustion and restore anti-tumor immunity. *J Exp Med* 2010; **207**: 2187–2194.
35 Hiroishi K, Tuting T, Tahara H, Lotze MT. Interferon-alpha gene therapy in combination with CD80 transduction reduces tumorigenicity and growth of established tumor in poorly immunogenic tumor models. *Gene Ther* 1999; **6**: 1988–1994.
36 Ishii S, Hiroishi K, Eguchi J, Hiraide A, Imawari M. Dendritic cell therapy with interferon-alpha synergistically suppresses outgrowth of established tumors in a murine colorectal cancer model. *Gene Ther* 2006; **13**: 78–87.
37 Yu P, Steel JC, Zhang M, Morris JC, Waldmann TA. Simultaneous blockade of multiple immune system inhibitory checkpoints enhances antitumor activity mediated by interleukin-15 in a murine metastatic colon carcinoma model. *Clin Cancer Res* 2010; **16**: 6019–6028.

Interleukin-4 and CpG oligonucleotide therapy suppresses the outgrowth of tumors by activating tumor-specific Th1-type immune responses

ATSUSHI KAJIWARA*, HIROYOSHI DOI*, JUNICHI EGUCHI, SHIGEAKI ISHII, AYAKO HIRAIDE-SASAGAWA, MASASHI SAKAKI, RISA OMORI, KAZUMASA HIROISHI and MICHIO IMAWARI

Division of Gastroenterology, Department of Medicine, Showa University School of Medicine, Tokyo 142-8666, Japan

Received November 14, 2011; Accepted January 9, 2012

DOI: 10.3892/or.2012.1723

Abstract. Because IL-4 and CpG oligodeoxynucleotides (CpG-ODNs) are immune stimulants, we evaluated the antitumor effects of IL-4 gene therapy and CpG-ODN treatment in a poorly immunogenic murine cancer model. We used a murine colorectal cancer MC38 cell line overexpressing the IL-4 gene (MC38-IL4). Incubation with MC38-IL4 and CpG-ODN enhanced bone marrow-derived dendritic cell (DC) maturation *in vitro*. In addition, interferon (IFN)-γ production was significantly increased in naïve splenocytes after they were coincubated with MC38-IL4 and CpG-ODN. When mice bearing MC38 wild-type tumors were inoculated subcutaneously with MC38-IL4 cells and CpG-ODN, the outgrowth of established parental tumors was significantly suppressed compared to those in the MC38-IL4-treated group (IL-4 vs. IL-4 + CpG-ODN, P=0.015). A marked infiltration of $CD8^+$ cells in the established parental tumors of mice treated with MC38-IL4 and CpG-ODN was confirmed by immunohistochemical analyses (MC38-IL4, 2.8±1.9 cells/field vs. MC38-IL4 + CpG-ODN, 20.7±15.3 cells/field, P=0.027). Significant tumor-specific cytolysis was detected when splenocytes of MC38-IL4 + CpG-ODN-treated mice were stimulated by γ-irradiated MC38-IL4 cells and CpG-ODN twice weekly *in vitro* and used as effector cells in a chromium-release assay (32.2±3.5% for MC38 cells vs. 3.2±1.1% for YAC-1 cells; at an effector to target ratio of 40). These results suggest that IL-4 and CpG-ODN treatment promotes potent Th1-type antitumor immune responses. Therefore, the combination of IL-4 gene therapy and CpG-ODN treatment for cancer should be evaluated in clinical trials.

Correspondence to: Dr Kazumasa Hiroishi, Division of Gastroenterology, Department of Medicine, Showa University School of Medicine, 1-5-8 Hatanodai, Shinagawa-ku, Tokyo 142-8666, Japan
E-mail: hiroishi@med.showa-u.ac.jp

*Contributed equally

Key words: interleukin-4, CpG, Th1, cytotoxic T lymphocyte, colorectal cancer

Introduction

Several original treatments of cancer have been developed in the last decade. Many anticancer drugs, including molecule-targeted drugs, have been applied clinically. Although some of these drugs have dramatically changed the prognoses of a number of diseases, several harmful side effects were observed. Because cancer immunotherapy is thought to induce few adverse events compared to other therapies, such as chemotherapy and radiation, the establishment of novel treatments that elicit potent immune responses against cancer has been anticipated. Indeed, many clinical trials of such treatments have been conducted. However, most of them have shown only minimal effects, and immunotherapy has not yet been applied as a conventional clinical treatment for cancer. Moreover, patients with advanced cancer exhibit impaired immune responses. Therefore, new strategies are needed to induce more potent antitumor immunities.

We have previously reported the antitumor effects and mechanisms of cell-based immunotherapies that were combined with treatments with cytokines, such as interferon (IFN)-α (1-3), IL-4 (4) and IL-12 (1). The administration of each cytokine gene-transduced tumor cells appears to induce potent cellular immune responses. However, the antitumor immune response mechanisms that were induced by these cytokine therapies differ from each other. In particular, we reported that IL-4 treatment resulted in unique and interesting biological effects.

IL-4, which is a type-2 response inducer (5,6), plays a major role in both B-cell and T-cell development in the immune system (7). In addition, it causes a class switch of B cells, upregulates MHC class II and adhesion molecules, and prevents the apoptosis of T cells (8). With respect to the antitumor effects, IL-4 has a direct inhibitory effect on tumor cell growth *in vivo* and *in vitro* (9,10) and an antiangiogenic effect (11). It has been reported that IL-4 activates endothelia in the tumor microenvironment, which results in an increased infiltration of immune cells (12). Other reports have suggested

that eosinophils and neutrophils are responsible for the antitumor effects induced by IL-4 (13-15). In addition, a recent study demonstrated that local IL-4 delivery at the site of vaccination activates local dendritic cells (DCs), which play a critical role in the initiation, promotion, and regulation of host immune responses and promote type-1 T-helper (Th1) cell responses (16). In that investigation, IL-4 appeared to support DC maturation and enhance IL-12p70 secretion from DCs. Because these findings support the therapeutic effects of IL-4 on tumors, IL-4 has been applied in the clinical treatment of tumors (17,18).

The potent immunomodulator CpG is present at the expected frequency of about 1 in 16 bases in bacterial DNA, but it is hardly observed in vertebrate DNA. It has been reported that DNA vaccines and synthetic oligodeoxynucleotides (ODN) containing an unmethylated CpG motif promote Th1-type immune responses. CpG stimulates DCs through the toll-like receptor 9 and enhances DC maturation, which may improve therapeutic effects on established tumors. Recently, we reported the synergistic effects of the combination of CpG-ODN and IFN-α on DC maturation (19). Furthermore, DC-based therapy with CpG-ODN and IFN-α exhibited potent antitumor effects by inducing tumor-specific cytotoxic T-lymphocyte (CTL) responses (3).

Although we have previously demonstrated that IL-4 promotes a Th1-type antitumor immune response, evidence of the induction of a more potent immune response that diminishes established tumors *in vivo* is required before justification of a clinical trial. In the present study, we anticipated that the combination of IL-4 gene therapy and CpG-ODN would have additive effects on tumors. Thus, we investigated the antitumor effects of the combination therapy and the underlying mechanisms of these effects in order to determine whether the combined therapy would be appropriated in a clinical trial.

Materials and methods

Mice. Female C57BL/6 (B6) mice that were 6-8 weeks old were purchased from Sankyo Lab Service (Tokyo, Japan) for use in experiments when they were 8-12 weeks old. Mice were maintained in an animal care facility at Showa University. This study was approved by the Ethics Committee for Animal Experiments of Showa University (permission #2011-1111).

Cell lines, culture medium and reagents. The MC38 murine colorectal adenocarcinoma cell line (B6 mouse origin) and the YAC-1 lymphoma cell line were maintained in RPMI-1640 medium that was supplemented with 10% heat-inactivated fetal calf serum, 2 mM L-glutamine, 100 IU/ml penicillin, and 100 μg/ml streptomycin (complete medium; CM) in a humidified incubator with 5% CO_2 in air at 37°C. All cell culture reagents were purchased from Life Technologies Corp. (Gaithersburg, MD). CpG-ODN-1826 and non-CpG-ODN-1911 (used as control ODN) were synthesized by Sigma-Aldrich Japan (Tokyo, Japan). We confirmed that non-CpG-ODN-1911 did not affect DC maturation or have antitumor activity (19).

Genetically modified tumor cell lines. The MC38 tumor cells that were transduced using retroviral vectors according to standard protocols, as previously described (20), were selected for antibiotic resistance in CM containing 0.5 mg/ml G418 (Sigma-Aldrich Corp., St. Louis, MO). We have established a IL-4-overexpressing MC38 cell line (MC38-IL4), which produces a large amount of IL-4 (359.9±108.2 ng/10^6 cells/48 h) (4). A neomycin-resistant gene-transduced MC38 (MC38-Neo) cell line was used as a control (21). The growth rate of the MC38-IL4 cells did not differ from those of MC38-wild-type (WT) or MC38-Neo cells *in vitro*.

Phenotypic changes of DCs after coincubation with IL-4-overexpressing tumor cells and CpG-ODN. In order to observe the immunogenic effects of IL-4 and CpG-ODN on DC maturation, flow cytometry was performed using FACSCalibur (Nippon Becton-Dickinson Co., Ltd., Tokyo, Japan). Bone marrow-derived DCs were generated, as previously reported (2). We incubated the DCs ($5x10^6$-$6x10^6$ cells/flask) with either MC38-IL4 or MC38-Neo cells ($1x10^6$ cells) that were 100 Gy-irradiated in combination with 6 μg/ml of either CpG-ODN-1826 or non-CpG-ODN-1911 *in vitro*. After a 24-h incubation, cells were harvested and stained with fluorescein isothiocyanate (FITC)-conjugated monoclonal antibodies. The monoclonal antibodies used in this assay were FITC-conjugated anti-H-2Kb, I-Ab, CD80, and CD86 antibodies (obtained from Nippon Becton-Dickinson). The results were shown as ratios of the mean fluorescent intensity (MFI) of the DCs that were incubated with each monoclonal antibody to the MFI of DCs incubated with the FITC-conjugated control IgG antibody.

IFN-γ and IL-10 production in naïve splenocytes coinoculated with IL-4-overexpressing tumor cells and CpG-ODN in vitro. In order to assess the effects of IL-4 and CpG-ODN on immune balance, we performed an enzyme-linked immunosorbent assay (ELISA) of the representative Th1-type cytokine, IFN-γ and the representative Th2-type cytokine, IL-10. Splenocytes ($1x10^6$ cells/ml) from naive mice were stimulated with either MC38-IL4 or MC38-Neo cells ($1x10^5$ cells/ml) either alone or in combination with 6 μg/ml of CpG-ODN-1826 or non-CpG-ODN-1911 *in vitro*. After a 24-h incubation, we measured the concentrations of IFN-γ and IL-10 in the supernatant of each culture with ELISA using a commercially available kit, according to the manufacturer's instructions (mouse IFN-γ ELISA and mouse IL-10 ELISA, Thermo Fisher Scientific, Inc., Rockford, IL). This experiment was repeated twice.

Combination therapy of IL-4-overexpressing tumors with CpG-ODN in therapeutic models. In order to evaluate the *in vivo* therapeutic effects of the combination of IL-4-overexpressing tumor cells and CpG-ODN on established tumors, we measured the size of established MC38-WT tumors in mice before and after treatment, as previously described (21). In brief, B6 mice were first injected s.c. with $3x10^5$ MC38-WT cells in the right flank. Seven, 9, and 11 days after the WT inoculation, $3x10^5$ MC38-Neo or MC38-IL4 cells were inoculated s.c. with 30 μg/mouse of either CpG-ODN-1826 or non-CpG-ODN-1911 around the established parental tumors, which had reached 4-20 mm^2 in size. Otherwise, tumor-bearing B6 mice ($5x10^5$ MC38-WT cells/mouse) were inoculated $5x10^5$ MC38-Neo or MC38-IL4 cells were inoculated s.c. with either CpG-ODN-1826 or ODN-1911 in the same